DYNAMIC ANALYSIS OF STRUCTURES WITH INTERVAL UNCERTAINTY

by

MEHDI MODARRESZADEH

Submitted in partial fulfillment of the requirements

For the degree of Doctor of Philosophy

Dissertation Advisor: Dr. Robert L. Mullen

Department of Civil Engineering

CASE WESTERN RESERVE UNIVERSITY

August, 2005

Dedicated to

my parents

for their live and support

TABLE OF CONTENTS

LIST OF TABLES

LIST OF FIGURES

ACKNOWLEDGEMENTS

The author expresses his deep and sincere gratitude to his academic advisor Prof. Robert L. Mullen for the perceptive instructions and support as well as motivation and encouragement that has inspired and nourished the author in numerous ways.

The author offers his deep appreciation to Prof. Dario A. Gasparini for the constant help, substantial guidance, and insightful suggestions.

The author is grateful to Prof. Daniela Calvetti, Prof. Arthur A. Huckelbridge, and Prof. Paul X. Bellini for providing their influential assistance.

LIST OF SYMBOLS

A	cross-sectional area
A	ordinary subset
$[A]$	symmetric matrix
$[\hat{A}]$	perturbed symmetric matrix
A_α	interval of confidence of (α) cut
c	viscous damping
$[C]$	global damping matrix
D_n	scaled modal coordinate
E	modulus of elasticity
E	referential set
$[E]$	perturbation matrix
$f(x)$	probability density function
$F_x(a)$	cumulative probability function
H	Hilbert space
i	imaginary number $(\sqrt{-1})$
$[I]$	identity matrix
K_n	generalized modal stiffness
$[K]$	global stiffness matrix
$[\overline{K}]$	deterministic element stiffness contribution to the global stiffness matrix
$[\widetilde{K}]$	interval global stiffness matrix
$[K_C]$	central stiffness matrix
$[K_e]$	stiffness matrix for a truss element
$[K_i]$	element stiffness matrix
$[\widetilde{K}_R]$	radial stiffness matrix
$[L_i]$	element Boolean connectivity matrix
$[L]$	matrix representation of $[A]$ on χ with respect to the basis $[X]$
M_n	generalized modal mass
$[M]$	global mass matrix
$[\overline{M}]$	deterministic element mass contribution to the global mass matrix
$[\widetilde{M}]$	interval element mass matrix
$[M_e]$	mass matrix for a truss element
$[M_i]$	element mass matrix

$p(t)$	external excitation
$[p]$	projection matrix
$P_n(t)$	generalized modal force
$\{P(t)\}$	vector of external excitation
$[P_i]$	projection matrix
$[Q]$	matrix of eigenvectors
$R(t)$	load effect
$R(x)$	Rayleigh quotient
$\Re$	real number domain
R_n	static modal load effect
$r\{\ddot{U}_g\}$	vector of rigid body pseudo-static displaced shape
$[T]$	linear operator in Sylvester's equation
$\mu_A(x)$	characteristic function defining the ordinary subset (A)
u	displacement field
$\dot{u}$	velocity field
$\ddot{u}$	acceleration field
$\{U\}$	vector of nodal displacement
$\{\dot{U}\}$	vector of nodal velocity
$\{\ddot{U}^t\}$	vector of nodal absolute acceleration motion
$\{\ddot{U}\}$	vector of nodal acceleration
$[X_i]$	matrix for representation of a subspace
$[\hat{X}_i]$	matrix for representation of a perturbed subspace
$y(t)$	modal coordinate
$\widetilde{Z}$	interval number
α	level of presumption
ε_i	interval of $[-1,1]$ for each element
η	test function
λ	eigenvalue
ζ_n	modal damping ratio
ρ	mass density
ϕ	interpolation function
$\{\varphi\}$	mode shape
χ	invariant subspace
ω	natural circular frequency
Γ	Domain of boundary conditions for truss elements
Γ_n	modal participation factor
$[\Lambda]$	diagonal matrix of eigenvalues
$[\Phi_2]$	matrix of complimentary eigenvectors to $\{\varphi_1\}$
$[\Omega_2]$	diagonal matrix of other natural circular frequencies

Dynamic Analysis of Structures with Interval Uncertainty

Abstract

by

MEHDI MODARRESZADEH

A new method for dynamic response spectrum analysis of a structural system with interval uncertainty is developed. This interval finite-element-based method is capable of obtaining the bounds on dynamic response of a structure with interval uncertainty. The proposed method is the first known method of dynamic response spectrum analysis of a structure that allows for the presence of any physically allowable interval uncertainty in the structure's geometric or material characteristics and externally applied loads other than Monte-Carlo simulation. The present method is performed using a set-theoretic (interval) formulation to quantify the uncertainty present in the structure's parameters such as material properties. Independent variations for each element of the structure are considered. At each stage of analysis, the existence of variation is considered as presence of the perturbation in a pseudo-deterministic system. Having this consideration, first, a linear interval eigenvalue problem is performed using the concept of monotonic behavior of eigenvalues for symmetric matrices subjected to non-negative definite perturbation which leads to a computationally efficient procedure to determine the bounds on a structure's natural frequencies. Then, using the procedures for perturbation of invariant subspaces of matrices, the bounds on directional deviation (inclination) of each mode shape are obtained.

Following this, the interval response spectrum analysis is performed considering the effects of input variation in terms of the structure's total response that includes maximum modal coordinates, modal participation factors and mode shapes. Using this method, it is shown that calculating the bounds on the dynamic response does not require a combinatorial solution procedure. Several problems that illustrate the behavior of the method and comparison with combinatorial and Monte-Carlo simulation results are presented.

CHAPTER I

INTRODUCTION

1.1 Analytical Background

The dynamic analysis of a structure is an essential procedure to design a reliable structure subjected to dynamic loads such as earthquake excitations. The objective of dynamic analysis is to determine the structure's response and interpret those theoretical results in order to design the structure. Dynamic response spectrum analysis is one of the methods of dynamic analysis which predicts the structure's response using the combination of modal maxima.

However, throughout conventional dynamic response spectrum analysis, the possible existence of any uncertainty present in the structure's geometric and/or material characteristics is not considered. In the design process, the presence of uncertainty is accounted for by considering a combination of load amplification and strength reduction factors that are obtained by modeling of historic data. However, the impact of presence of uncertainty on a design is not considered in the current deterministic dynamic response spectrum analysis. In the presence of uncertainty in the geometric and/or material properties of the system, an uncertainty analysis must be performed to obtain bounds on the structure's response.

Uncertainty analysis on the dynamics of a structure requires two major considerations: first, modifications on the representation of the characteristics due to the existence of uncertainty and second, development of schemes that are capable of considering the presence of uncertainty throughout the solution process. Those developed schemes must be consistent with the system's physical behavior and also be computationally feasible.

The set-theoretic (unknown but bounded) or interval representation of vagueness is one possible method to quantify the uncertainty present in a physical system. The interval representation of uncertainty in the parametric space has been motivated by the lack of detailed probabilistic information on possible distributions of parameters and/or computational issues in obtaining solutions.

In this work, a new method for dynamic response spectrum analysis of a structural system with interval uncertainty entitled Interval Response Spectrum Analysis (IRSA) is developed. IRSA enhances the deterministic dynamic response spectrum analysis by including the presence of uncertainty at each step of the analysis procedure. In this finite-element-based method, uncertainty in the elements is viewed by a closed set-representation of element parameters that can vary within intervals defined by extreme values. This representation transforms the point values in the deterministic system to inclusive sets of values in the system with interval uncertainty.

The concepts of matrix perturbation theories are used in order to find the bounds on the intervals of the terms involved in the modal contributions to the total structure's response including: circular natural frequencies, mode shapes and modal coordinates.

Having the bounds on those terms, the bounds on the total response are obtained using interval calculations. Functional dependency and independency of intervals of uncertainty are considered in order to attain sharper results. The IRSA can calculate the bounds on the dynamic response without combinatorial or Monte-Carlo simulation procedures. This computational efficiency makes IRSA an attractive method to introduce uncertainty into dynamic analysis.

This work represents the synthesis of two historically independent fields, structural dynamics and interval analysis. In order to represent the background for this work, a review of development of both fields is presented.

1.2 Dissertation Overview

In chapter II, the analytical procedure for deterministic dynamic analysis is presented. Chapter III is devoted to fundamentals of uncertainty analyses with emphasis on the interval method. In chapter IV, matrix perturbation theories for eigenvalues and eigenvectors are discussed. Chapter V introduces the method of interval response spectrum analysis. In chapter VI, the bounds on variations of natural frequencies and mode shapes are obtained. Chapter VII is devoted to determination of the bounds on the total response of the structure. In chapter VIII, exemplars and numerical results are presented. Chapter IX is devoted to observations and conclusions.

CHAPTER II

CONVENTIONAL DETERMINISTIC DYNAMIC ANALYSIS

2.1 Structural Dynamics Historical Background

Modern theories of structural dynamics were introduced mostly in mid 20^{th} century. M. A. Biot (1932) introduced the concept of earthquake response spectra and G. W. Housner (1941) was instrumental in the widespread acceptance of this concept as a practical means of characterizing ground motions and their effects on structures. N. M. Newmark (1952) introduced computational methods for structural dynamics and earthquake engineering. In 1959, he developed a family of time-stepping methods based on variation of acceleration over a time-step.

A. W. Anderson (1952) developed methods for considering the effects of lateral forces on structures induced by earthquake and wind and C. T. Looney (1954) studied the behavior of structures subjected to forced vibrations. Also, D. E. Hudson (1956) developed techniques for response spectrum analysis in engineering seismology. A. Veletsos (1957) determined natural frequencies of continuous flexural members. Moreover, he investigated the deformation of non-linear systems due to dynamic loads. E. Rosenblueth (1959) introduced methods for combining modal responses and characterizing earthquake analysis.

J. Biggs (1964) developed dynamic analyses for structures subjected to blast loads. Moreover, numerical methods for dynamics of structures and modal analysis were further developed by J. Penzien and R. W. Clough (1993).

2.2 Equation of Motion

In the development of IRSA, the truss element is used as the exemplar for a more general finite element analysis. Other than the details of interval parameterization of the resulting element matrices, the proposed method of IRSA should extend to a general finite element analysis.

Considering the partial differential equation of motion for a truss element:

$$(EAu_{,x})_{,x} - c\dot{u} - \rho\ddot{u} + p(t) = 0 \tag{2.1}$$

$$\text{with B.C.}: \; u = g \;\; on \;\; \Gamma_1 \;, \;\; EAu_{,x} = p \;\; on \;\; \Gamma_2$$

in which, E is the modulus of elasticity, A is the cross-sectional area, c is the viscous damping, ρ is the mass density and $p(t)$ is the external excitation. The terms $u, \dot{u}$ and $\ddot{u}$ are the displacement field and its temporal derivatives, respectively; and, x is the spatial variable.

Multiplying by a test function (η) in spatial domain in order to find $(u \in H_g^2 \;\forall \eta \in H_o^0)$, in which H is the Hilbert space, Eq. (2.1) becomes:

$$\int_{\Omega} \eta[(EAu_{,x})_{,x} - c\dot{u} - \rho\ddot{u} + p(t)]dxdt + B.C. = 0 \tag{2.2}$$

Integrating by parts to obtain the symmetric weak form to find $(u \in H_g^1 \;\; \forall \eta \in H_o^1)$ yields:

$$\int_\Omega [\eta_{,x} EAu_{,x} + \eta c\dot{u} + \eta\rho\ddot{u} - \eta p(t)] dxdt + B.C. = 0 \tag{2.3}$$

The spatial domain of displacement field and the test function can be semi-discretized by approximating the functions u and η in space over each element by linear interpolation functions as:

$$u(x,t) = \sum_I \phi_I(x) u_I(t) \tag{2.4}$$

$$\eta(x,t) = \sum_I \phi_I(x) \eta_I(t) \tag{2.5}$$

in which:

$$\{\phi(x)\}^T = \begin{Bmatrix} \dfrac{L-x}{L} & \dfrac{x}{L} \end{Bmatrix} \tag{2.6}$$

Substituting the above relationships over the elements yields:

$$\begin{aligned} &\sum_{Element} \int_\Omega \Big([L]^T \{\phi\} \rho \{\phi\}^T [L] \{\ddot{U}\} + [L]^T \{\phi\} c \{\phi\}^T [L] \{\dot{U}\} + \ldots \\ &[L]^T \{\phi_{,x}\} EA \{\phi_{,x}\}^T [L] \{U\} - [L]^T \{\phi\} p(t) \Big) d\Omega + B.C. = \{0\} \end{aligned} \tag{2.7}$$

where, $\{U\}$ is the vector of nodal displacement, $\{\dot{U}\}$ is the vector of nodal velocity, $\{\ddot{U}\}$ is the vector of nodal acceleration, the vector $\{P(t)\}$ is the nodal external excitation and $[\,L\,]$ is the Boolean connectivity matrix.

Integrating over the domain, the equation of motion for vibration of a multiple degree of freedom (DOF) system is defined as a linear system of ordinary differential equations as:

$$[M]\{\ddot{U}\}+[C]\{\dot{U}\}+[K]\{U\}=\{P(t)\} \tag{2.8}$$

where, $[M_{n\times n}]$, $[C_{n\times n}]$, and $[K_{n\times n}]$ are the global mass, global damping and global stiffness matrices, respectively.

Stiffness and Mass Matrices for a Truss Element

The stiffness, consistent mass and lumped mass matrices for a linear truss element are as following, respectively.

$$[K_e]=\frac{EA}{L}\begin{bmatrix}+1 & -1\\ -1 & +1\end{bmatrix} \qquad [M_e]^C=\frac{\rho AL}{6}\begin{bmatrix}2 & 1\\ 1 & 2\end{bmatrix} \qquad [M_e]^L=\frac{\rho AL}{2}\begin{bmatrix}1 & 0\\ 0 & 1\end{bmatrix}$$

Solution to Equation of Motion

The solution of Eq.(2.8) can be divided into homogenous and particular parts. In fact, the homogenous part is the solution to the free vibration of the system and the particular part is the solution to the system’s forced vibration. Thus, in order to obtain the solution to Eq.(2.8), the following procedure can be used.

2.3 Free Vibration

The equilibrium equations for the free vibration of an undamped multiple degree of freedom system are defined as a set of linear homogeneous second-order ordinary differential equations as:

$$[M]\{\ddot{U}\} + [K]\{U\} = \{0\} \tag{2.9}$$

Assuming a harmonic motion for the temporal displacement ($\{U\} = \{\varphi\}e^{i\omega t}$), Eq.(2.9) is transformed to a set of linear homogeneous algebraic equations as:

$$([K] - (\omega^2)[M])\{\varphi\} = \{0\} \tag{2.10}$$

or:

$$[K]\{\varphi\} = (\omega^2)[M]\{\varphi\} \tag{2.11}$$

Eq.(2.10) is known as a generalized eigenvalue problem between the stiffness and mass matrices of the system.

The values of (ω) are the natural circular frequencies and the vectors {φ} are the corresponding mode shapes.

<u>Solution to Eigenvalue Problem</u>

For non-trivial solutions, the determinant of $([K] - (\omega^2)[M])$ must be zero. This leads to a scalar equation, known as the characteristic equation, whose roots are the system's natural circular frequencies of the system (ω).

Substituting each value of circular frequency in Eq.(2.10) yields a corresponding eigenvector or mode shape that is defined to an arbitrary multiplicative constant. The modal matrix $\left[\{\varphi_1\} \quad ... \quad \{\varphi_N\}\right]$ spans the N-dimensional linear vector space.

This means that the eigenvectors $\{\varphi_1\} \quad ... \quad \{\varphi_N\}$ form a complete basis, i.e., any vector such as the vector of dynamic response of a multiple degree of freedom (MDOF) system, $\{U(t)\}$, can be expressed as a linear combination of the mode shapes:

$$\{U(t)\} = \{\varphi_1\}.y_1(t) + \{\varphi_2\}.y_2(t) + ... + \{\varphi_N\}.y_N(t) = \sum_{n=1}^{N} \{\varphi_n\}.y_n(t) \qquad (2.12)$$

in which, the terms $y_n(t)$ are modal coordinates and therefore, $\{U(t)\}$ is defined in modal coordinate space, since the values of $\{\varphi\}$ are independent of time for linear systems, Eq. (2.11).

Furthermore, the temporal derivatives of total response can be expressed as:

$$\{\dot{U}(t)\} = \{\varphi_1\}.\dot{y}_1(t) + \{\varphi_2\}.\dot{y}_2(t) + ... + \{\varphi_N\}.\dot{y}_N(t) = \sum_{n=1}^{N} \{\varphi_n\}.\dot{y}_n(t) \qquad (2.13)$$

$$\{\ddot{U}(t)\} = \{\varphi_1\}.\ddot{y}_1(t) + \{\varphi_2\}.\ddot{y}_2(t) + ... + \{\varphi_N\}.\ddot{y}_N(t) = \sum_{n=1}^{N} \{\varphi_n\}.\ddot{y}_n(t) \qquad (2.14)$$

which are also defined in modal coordinate space.

Orthogonality of Modes

Considering the generalized eigenvalue problem for the m^th and n^th circular frequencies and corresponding mode shapes:

$$([K]-(\omega_m^2)[M])\{\varphi_m\}=\{0\} \tag{2.15}$$

$$([K]-(\omega_n^2)[M])\{\varphi_n\}=\{0\} \tag{2.16}$$

Pre-multiplying Eq.(2.15) and Eq.(2.16) by $\{\varphi_n\}^T$ and $\{\varphi_m\}^T$, respectively:

$$\{\varphi_n\}^T[K]\{\varphi_m\}-(\omega_m^2)\{\varphi_n\}^T[M]\{\varphi_m\}=0 \tag{2.17}$$

$$\{\varphi_m\}^T[K]\{\varphi_n\}-(\omega_n^2)\{\varphi_m\}^T[M]\{\varphi_n\}=0 \tag{2.18}$$

Then, transposing Eq (2.18) and invoking the symmetric property of the $[K]$ and $[M]$ matrices yields:

$$\{\varphi_n\}^T[K]\{\varphi_m\}-(\omega_n^2)\{\varphi_n\}^T[M]\{\varphi_m\}=0 \tag{2.19}$$

Subtracting Eq.(2.19) from Eq.(2.17) yields:

$$\left((\omega_m^2)-(\omega_n^2)\right)\{\varphi_n\}^T[M]\{\varphi_m\}=0 \tag{2.20}$$

For any $(m\neq n)$, if $(\omega_m^2\neq\omega_n^2)$:

$$\{\varphi_n\}^T[M]\{\varphi_m\}=0 \tag{2.21}$$

$$\{\varphi_n\}^T[K]\{\varphi_m\}=0 \tag{2.22}$$

Eqs.(2.21,2.22) express the characteristic of “orthogonality” of mode shapes with respect to mass and stiffness matrices, respectively.

2.4 Forced Vibration

The equation of motion for forced vibration of an undamped MDOF system is defined as:

$$[M]\{\ddot{U}\} + [K]\{U\} = \{P(t)\} \tag{2.23}$$

Expressing displacements and their time derivatives in modal coordinate space:

$$\sum_{n=1}^{N}[M]\{\varphi_n\}\ddot{y}_n(t) + \sum_{n=1}^{N}[K]\{\varphi_n\}y_n(t) = \{P(t)\} \tag{2.24}$$

Premultiplying each term in Eq.(2.24) by $\{\varphi_n\}^T$:

$$\sum_{n=1}^{N}\{\varphi_n\}^T[M]\{\varphi_n\}\ddot{y}_n(t) + \sum_{n=1}^{N}\{\varphi_n\}^T[K]\{\varphi_n\}y_n(t) = \{\varphi_n\}^T\{P(t)\} \tag{2.25}$$

Invoking orthogonality, Eq.(2.24) is reduced to a set of N uncoupled modal equations as:

$$\{\varphi_n\}^T[M]\{\varphi_n\}\ddot{y}_n(t) + \{\varphi_n\}^T[K]\{\varphi_n\}y_n(t) = \{\varphi_n\}^T\{P(t)\} \tag{2.26}$$

or:

$$M_n\ddot{y}_n(t) + K_n y_n(t) = P_n(t) \tag{2.27}$$

where, $M_n = \{\varphi_n\}^T[M]\{\varphi_n\}, K_n = \{\varphi_n\}^T[K]\{\varphi_n\}$ and $P_n(t) = \{\varphi_n\}^T\{P(t)\}$ are generalized modal mass, generalized modal stiffness and generalized modal force, respectively. Dividing by modal mass M_n and adding the assumed modal damping ratio (ζ_n), Eq.(2.27) becomes:

$$\ddot{y}_n(t) + (2\zeta_n\omega_n)\dot{y}_n(t) + (\omega_n^2)y_n(t) = \frac{P_n(t)}{M_n} \tag{2.28}$$

Proportional Excitation

If loading is proportional $\{P(t)\} = \{P\}p(t)$, meaning the applied forces have the same time variation defined by $p(t)$ (such as ground motion), Eq.(2.28) can be expressed as:

$$\ddot{y}_n(t) + (2\zeta_n\omega_n)\dot{y}_n(t) + (\omega_n^2)y_n(t) = \frac{\{\varphi_n\}^T\{P\}}{M_n}\left(p(t)\right) \tag{2.29}$$

Defining a modal participation factor, Γ_n, as:

$$\Gamma_n = \frac{\{\varphi_n\}^T\{P\}}{M_n} = \frac{\{\varphi_n\}^T\{P\}}{\{\varphi_n\}^T[M]\{\varphi_n\}} \tag{2.30}$$

Also defining a scaled generalized modal coordinate:

$$D_n(t) = \frac{y_n(t)}{\Gamma_n} \tag{2.31}$$

Eq.(2.28) is rewritten in terms of the scaled modal coordinate $(D_n(t))$ as:

$$\ddot{D}_n(t) + (2\zeta_n\omega_n)\dot{D}_n(t) + (\omega_n^2)D_n(t) = p(t) \tag{2.32}$$

Therefore, using modal decomposition, the equation of motion for an *N*-DOF system is uncoupled to *N* equations of motion of generalized single degree of freedom (SDOF) systems.

2.4.1 Response History Analysis

In response history analysis (RHA), N uncoupled SDOF modal equations, Eq.(2.32), are solved for the modal coordinates $(D_n(t))$, and then, by superposing the modal responses, the total displacement response of the system is obtained as:

$$U(t) = \sum_{n=1}^{N} (D_n(t))(\Gamma_n)\{\varphi_n\} \tag{2.33}$$

in which the "time history" of the total response is obtained by the summation of modal responses as products of time history of modal coordinates $(D_n(t))$, modal participation factors (Γ_n), and modal displacements (mode shapes) $\{\varphi_n\}$. Moreover, the time history of any load effect, $R(t)$, may be expressed as:

$$R(t) = \sum_{n=1}^{N} (D_n(t))(\Gamma_n)\{R_n\} \tag{2.34}$$

in which, $\{R_n\}$ is a static modal load effect.

2.4.2 Response Spectrum Analysis

In response spectrum analysis (RSA), for each uncoupled generalized SDOF modal equation, Eq.(2.32), the maximum modal coordinate $(D_{n,\max})$ is obtained using the response spectrum of the external excitation $p(t)$ and assumed modal damping ζ_n (Figure(1)).

Response spectra are found by obtaining the maximum dynamic amplification (maximum ratio of dynamic to static responses) for a set of natural frequencies.

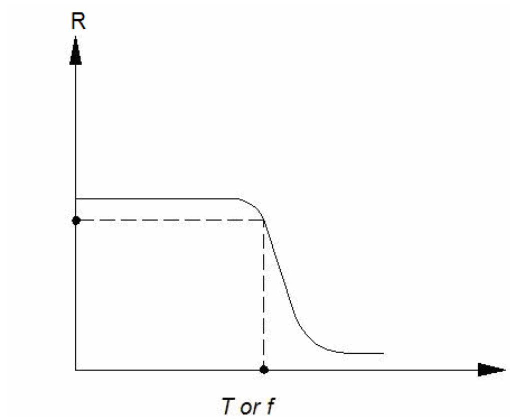

Figure (1): A generic response spectrum for an external excitation $p(t)$

Therefore, the modal response is obtained as:

$$\{U_{n,\max}\} = (D_{n,\max})(\Gamma_n)\{\varphi_n\} \tag{2.35}$$

Superposition of modal maxima

The total response is obtained using superposition of modal maxima. The superposition can be performed by summation of absolute values of modal responses.

$$\{U_{\max}\} = \sum_{n=1}^{N} \left|U_{n,\max}\right| \tag{2.36}$$

which provides a conservative estimate of the maximum response. As an approximation, the method of Square Root of Sum of Squares (SRSS) of modal maxima can be used when natural frequencies are distinct (Rosenblueth 1959):

$$\{U_{\max}\} = \sqrt{\sum_{n=1}^{N} \{U_{n,\max}^2\}} \tag{2.37}$$

Also, the method of complete quadratic combination (CQC) can be used.

Ground Excitation- Response Spectrum Analysis

The equation of motion for an undamped MDOF system subjected to ground excitation (support motion) from an earthquake is:

$$[M]\{\ddot{U}^t\}+[K]\{U\}=\{0\} \tag{2.38}$$

where $\{\ddot{U}^t\}$ is the vector of absolute acceleration. The vector $\{U\}$ is defined as the relative displacement vector, defined as:

$$\{U\}=\{U^t\}-\{r\}(U_g) \tag{2.39}$$

where $\{r\}U_g$ is the vector of rigid body pseudo-static displaced shape due to horizontal ground motion. Substituting Eq.(2.39) in Eq.(2.38) yields:

$$[M]\{\ddot{U}\}+[K]\{U\}=-[M]\{r\}\ddot{U}_g \tag{2.40}$$

As before, solving the linear eigenvalue problem, defining the response in modal coordinate space, uncoupling and adding assumed modal damping yields:

$$\ddot{y}_n(t)+(2\zeta_n\omega_n)\dot{y}_n(t)+(\omega_n^2)y_n(t)=-\frac{\{\varphi_n\}^T[M]\{r\}}{\{\varphi_n\}^T[M]\{\varphi_n\}}\ddot{U}_g \tag{2.41}$$

Defining the modal participation factor, Γ_n, as:

$$\Gamma_n=\frac{\{\varphi_n\}^T[M]\{r\}}{\{\varphi_n\}^T[M]\{\varphi_n\}} \tag{2.42}$$

Also, defining the scaled generalized modal coordinate $D_n(t) = y_n(t)/\Gamma_n$, Eq.(2.40) may be rewritten in terms of the scaled modal coordinate $(D_n(t))$ as:

$$\ddot{D}_n(t) + (2\zeta_n \omega_n)\dot{D}_n(t) + (\omega_n^2)D_n(t) = -\ddot{U}_g \qquad (2.43)$$

Performing response spectrum analysis for ground excitation, for each uncoupled generalized SDOF modal equation, Eq.(2.43), the maximum modal response is obtained using earthquake response spectra such as the Newmark Blume Kapur (NBK) design spectra (Figure(2)).

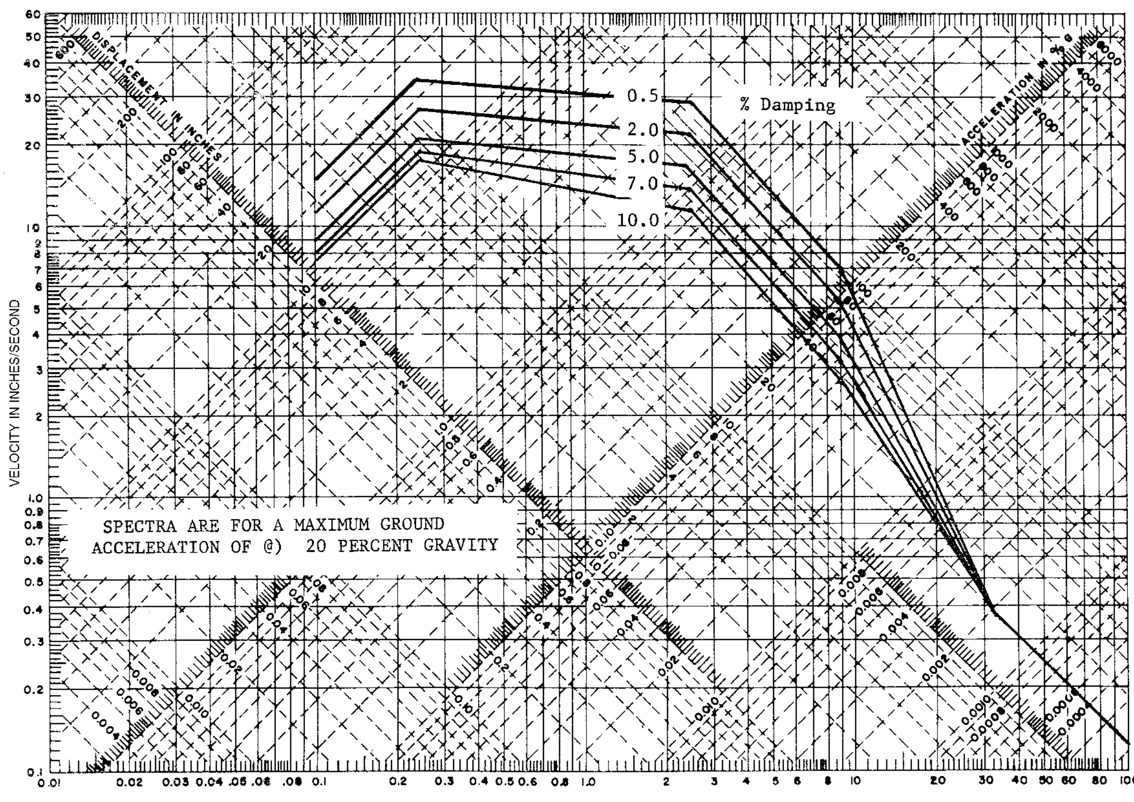

Figure (2): NBK design spectra (Newmark, Blume and Kapur 1973)

Therefore, the maximum modal coordinate is obtained as:

$$D_{n,\max} = S_d(\omega_n, \zeta_n) \tag{2.44}$$

The total response is obtained using superposition of modal maxima. The superposition is performed by considering Square Root of Sum of Squares (SRSS) of modal maxima:

$$\{U_{\max}\} = \sqrt{\sum_{n=1}^{N} D_{n,\max}^2 \Gamma_n^2 \{\varphi_n^2\}} \tag{2.45}$$

2.5 Response Spectrum Analysis Summary

Response spectrum analysis to compute the dynamic response of a MDOF to external forces and ground excitation can be summarized as a sequence of steps as:

1. Define the structural properties.
    - Determine the stiffness matrix $[K]$ and mass matrix $[M]$.
    - Assume the modal damping ratio ζ_n.
2. Perform a generalized eigenvalue problem between the stiffness and mass matrices.
    - Determine natural circular frequencies (ω_n).
    - Determine mode shapes $\{\varphi_n\}$.

3. Compute the maximum modal response.

- Determine the maximum modal coordinate $D_{n,\max}$ using the excitation response spectrum for the corresponding natural circular frequency and modal damping ratio.
- Determine the modal participation factor Γ_n.
- Compute the maximum modal response as a product of maximum modal coordinate, modal participation factor and mode shape.

4. Combine the contributions of all maximum modal responses to determine the maximum total reponse using SRSS or other combination methods.

<u>Limitations</u>

In the presence of uncertainty in the structure's physical or geometrical parameters, the deterministic structural dynamic analysis cannot be performed and hence, a new method must be developed to incorporate an uncertainty analysis into the conventional response spectrum analysis.

CHAPTER III

UNCERTAINTY ANALYSIS FUNDAMENTALS

3.1 Background

In structural engineering, design of an engineered system requires that the performance of the system is guaranteed over its lifetime. However, the parameters for designing a reliable structure possess physical and geometrical uncertainties. The presence of uncertainty can be attributed to physical imperfections, model inaccuracies and system complexities. Moreover, neither the initial conditions, nor external forces, nor the constitutive parameters can be perfectly described. Therefore, in order to design a reliable structure, the possible uncertainties in the system must be included in the analysis procedures.

Categories of Uncertainty

The concept of uncertainty can be divided into two major categories:

- Aleatory: The system has an intrinsic random or stochastic nature and it is not predictable.
- Epistemic: The uncertainty induced by the lack of knowledge and it is predictable.

Example of aleatory uncertainty is the behavior of photons in quantum mechanics where there is no hidden variable in the model or missing information.

Epistemic systems have uncertainty that may be reduced upon additional information. Uncertainty in the stiffness of a structural member may be reduced by measurement of the element behavior.

Aleatory uncertainty assumes that an underlying probability density function (PDF) exists and is the square of the wave function in quantum mechanics and also, the PDF is a fundamental property of the system.

In most engineering systems, the PDF is obtained from historic data and represents both epistemic and aleatory uncertainties. Thus, the precise form of a PDF can only be assumed. On the other hand, interval methods play an important role in quantifying epistemic uncertainty.

Deterministic analysis

In deterministic analysis of physical systems, defining the system's characteristics as point quantities, using conventional deterministic algebraic values, is sufficient to model the system and perform the analysis (Figure(3)).

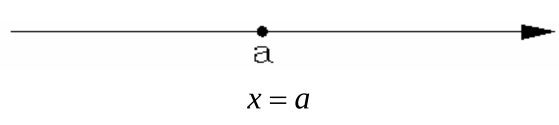

Figure (3): A deterministic algebraic variable

3.2 Uncertainty Analysis

In order to perform uncertainty analysis on a physical system, the uncertainty present in the system's physical characteristics must be fully mathematically quantified. Presently, there are three paradigms to consider uncertainty in non-deterministic structural analysis:

<u>1. Stochastic analysis</u>

In stochastic analysis, the theory of probability which was developed based on aleatory uncertainty. Extensions have been made such as "degree of belief" probability on subjective probability which includes epistemic effects.

<u>2. Fuzzy analysis</u>

In fuzzy analysis, the theory of possibility for fuzzy sets is used which assumes epistemic uncertainty.

<u>3. Interval analysis</u>

In interval analysis, the theory of convex (interval) sets is used which assumes epistemic or aleatory uncertainties (such as Dempster-Shafer bounds that are epistemic bounds on aleatory probability functions).

3.3 Stochastic Analysis

The stochastic approach to uncertain problems is to model the structural parameters as random quantities (Pascal 1654). Therefore, all information about the structural parameters is provided by the probability density functions. This probability density function is then used to determine an estimate of the system's behavior.

Random Variable

A random quantity, used in stochastic analysis, is defined by a deterministic function that yields the probability of existence of the random variable in a given subset of the real space (Figure (4)), (Eq.(3.1)):

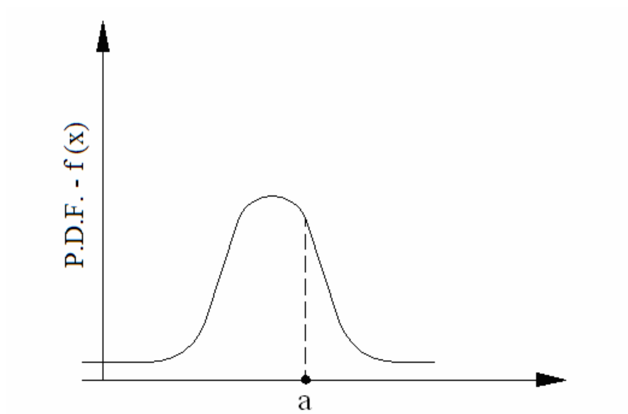

Figure (4): Probability density function of a random quantity

$$F_x(a) = P([x \le a]) = \int_{-\infty}^{a} f(x)dx \tag{3.1}$$

in which, $F_x(a)$ is cumulative probability distribution function evaluated for random variable (a) and $f(x)$ is the corresponding probability density function.

3.4 Fuzzy Analysis

The fuzzy approach to the uncertain problems is to model the structural parameters as fuzzy quantities (Lotfi-zadeh 1965). In conventional set theories, either an element belongs or doesn't belong to set. However, fuzzy sets have a membership function that allows for "partial membership" in the set. Using this method, structural parameters are quantified by fuzzy sets. Following fuzzifying the parameters, structural analysis is performed using fuzzy operations.

<u>Fuzzy Subset</u>

Considering *E* as a referential set in $\Re$, an ordinary subset *A* of the referential set is defined by its characteristic function $\mu_A(x)$ as:

$$\forall x \in E : \mu_A(x) \in \{0,1\} \tag{3.2}$$

which exhibits whether or not, an element of *E* belongs to the ordinary subset *A*. For the same referential set *E*, a fuzzy subset *A* is defined by its characteristic function, membership function $\mu_A(x)$, as:

$$\forall x \in E : \mu_A(x) \in [0,1] \tag{3.3}$$

A fuzzy number is defined by its membership function whose domain is $\Re$ while its range is bounded between [0,1]. The domain of the membership function is known as the interval of confidence and the range is known as the level of presumption.

Therefore, each level of presumption α (α-cut membership, $\alpha \in [0,1]$) has a unique interval of confidence $A_\alpha = [a^\alpha, b^\alpha]$, which is a monotonic decreasing function of α (Figure(5)), (Eqs. (3.4,3.5)):

$$\forall \alpha_1, \alpha_2 \in [0,1], (\alpha_1 > \alpha_2) \Rightarrow A_{\alpha_1} \subset A_{\alpha_2} \tag{3.4}$$

or:

$$\forall \alpha_1, \alpha_2 \in [0,1], (\alpha_1 > \alpha_2) \Rightarrow [a^{\alpha_1}, b^{\alpha_1}] \subset [a^{\alpha_2}, b^{\alpha_2}] \tag{3.5}$$

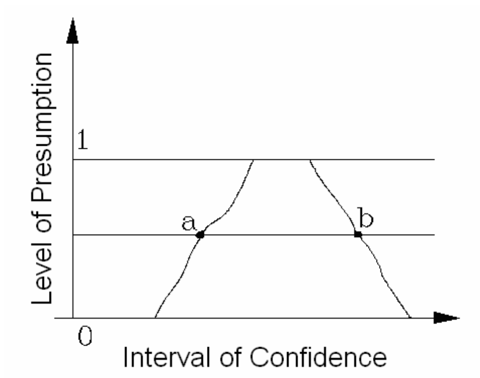

Figure (5): Membership function of a fuzzy quantity

3.5 Interval Analysis

The interval approach to the uncertain problems is to model the structural parameters as interval quantities. In this method, uncertainty in the elements is viewed by a closed set-representation of element parameters that can vary within intervals between extreme values. Then, structural analysis is performed using interval operations.

Interval Analysis Historical Background

The concept of representation of an imprecise real number by its bounds is quite old. In fact, Archimedes (287-212 B.C.) defined the irrational number (π) by an interval $3\frac{10}{71} < \pi < 3\frac{1}{7}$, which he found by approximating the circle with the inscribed and circumscribed 96-side regular polygons. Early work in modern interval analysis was performed by W. H. Young (1908), who introduced functions with values which are bounded between extreme limits. The concept of operations with a set of multi-valued numbers was introduced by R. C. Young (1931), who developed a formal algebra of multi-valued numbers. Also, the special case of multi-valued functions with closed intervals was discussed by Dwyer (1951). The introduction of digital computers in the 1950's provided impetus for further interval analysis as discrete representations of real numbers with associated truncation error.

Interval mathematics was further developed by Sunaga (1958) who introduced the theory of *interval algebra* and its applications in numerical analysis. Also, R. Moore (1966) introduced *interval analysis*, interval vectors and interval matrices as a set of techniques that provides error analyses for computational results.

Interval analysis provides a powerful set of tools with direct applicability to important problems in scientific computing. Alefeld and Herzberger (1983) presented an extensive treatment of interval linear and non-linear algebraic equations and interval methods for systems of equations. Moreover, Neumaier (1990) investigated the methods for solution of interval systems of equations.

The concept of interval systems has been further developed in analysis of structures with interval uncertainty. Muhanna and Mullen (1999) developed fuzzy finite-element methods for solid mechanics problems. For the solution of interval finite element method (IFEM) problems, Muhanna and Mullen (2001) introduced an Element-by-Element interval finite element formulation, in which a guaranteed enclosure for the solution of interval linear systems of equations was achieved.

The research in interval eigenvalue problem began to emerge as its wide applicability in science and engineering was realized. Dief (1991) presented a method for computing interval eigenvalues of an interval matrix based on an assumption of invariance properties of eigenvectors. Using Dief's method, the lower eigenvalues have a wider range of uncertainty than the exact results.

The concept of the interval eigenvalue problem has been developed in dynamics of structures with uncertainty. Qiu, Chen and Elishokoff (1995) have introduced a method to find the bounds on eigenvalues. In their work, the perturbation of the eigenvalue is derived from pre and post multiplying the perturbed matrix by the exact eigenvector which is inconsistent with matrix perturbation theories.

However, since the presence of perturbation in the matrix results in perturbation of both eigenvalues *and* eigenvectors, applying the unperturbed eigenvector to determine the perturbation of the eigenvalue may lead to incorrect results. The second problem in this work solves the problem cited by Qiu, Chen and Elishokoff (1995) for exact bounds with the present scheme and illustrates the difference in solution.

Qiu, Chen and Elishokoff (1996) have introduced an alternate method for bounding the natural frequencies of a structural system. However, their results are wider than sharp values because of a non-parametric formulation and the existence of variation inside the matrices. Moreover, their definition of the concept of maximin characterization appears to be inconsistent with the formal mathematical definitions. The constraint-induced subspaces in this concept are not completely arbitrary but they should be orthogonal to arbitrary vectors (Bellman 1960 and Strang 1976). The third problem in the present work solves the problem cited by Qiu, Chen and Elishokoff (1996) with the present scheme and compares the results.

As part of the present work, Modares and Mullen (2004) have introduced a method for the solution of the parametric interval eigenvalue problem resulting from semi-discretization of structural dynamics which determines the exact bounds of the natural frequencies of a structure.

Interval (Convex) Number

A real interval is a closed set defined by extreme values as (Figure(6)):

$$\tilde{Z} = [z^l, z^u] = \{z \in \Re \mid z^l \le z \le z^u\} \tag{3.6}$$

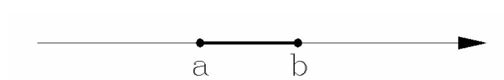

$$\tilde{x} = [a, b]$$

Figure (6): An interval quantity

One interpretation of an interval number is a random variable whose probability density function is unknown but non-zero only in the range of interval.

Another interpretation of an interval number includes intervals of confidence for α-cuts of fuzzy sets. This interval representation transforms the point values in the deterministic system to inclusive set values in the system with bounded uncertainty.

Interval Arithmetic Operations

Interval arithmetic is a computational tool that can be used to represent uncertainty as:

1. A set of probability density functions.
2. In Dempster-Shafer models for epistemic probability.
3. α - cuts in fuzzy sets.

In this work, the symbol (~) represents an interval quantity. Considering $\widetilde{X} = [a, b]$ and $\widetilde{Y} = [c, d]$ as two interval numbers, the basic interval arithmetic operations are:

Addition:

$$\widetilde{X} + \widetilde{Y} = [a + c, b + d] \tag{3.7}$$

Subtraction:

$$\widetilde{X} - \widetilde{Y} = [a - d, b - c] \tag{3.8}$$

Multiplication by scalar:

$$\beta \times \widetilde{X} = [\min(\beta a, \beta b), \max(\beta a, \beta b),] \tag{3.9}$$

Multiplication:

$$\widetilde{X} \times \widetilde{Y} = [\min(ac, ad, bc, bd), \max(ac, ad, bc, bd)] \tag{3.10}$$

Properties of Interval Multiplication:

Associative:

$$\widetilde{X} \times \widetilde{Y} = \widetilde{Y} \times \widetilde{X} \tag{3.11}$$

Commutative:

$$\widetilde{X} \times (\widetilde{Y} \times \widetilde{Z}) = (\widetilde{X} \times \widetilde{Y}) \times \widetilde{Z} \tag{3.12}$$

Distributive:

$$\widetilde{X} \times (\widetilde{Y} + \widetilde{Z}) \subset \widetilde{X} \times \widetilde{Y} + \widetilde{X} \times \widetilde{Z} \tag{3.13}$$

Therefore, the distributive property of interval multiplication is weaker than that in conventional algebra and it is one possible cause of loss of sharpness in interval operations.

Division:

$$\frac{\widetilde{X}}{\widetilde{Y}} = [a,b] \times [\frac{1}{d}, \frac{1}{c}], (0 \notin [c,d]) \tag{3.14}$$

Interval Vector (2-D):

$$\widetilde{V} = \begin{Bmatrix} \widetilde{X} \\ \widetilde{Y} \end{Bmatrix} = \begin{Bmatrix} [a,b] \\ [c,d] \end{Bmatrix} \tag{3.15}$$

which represents a "box" in 2-D space as the enclosure (Figure(7)).

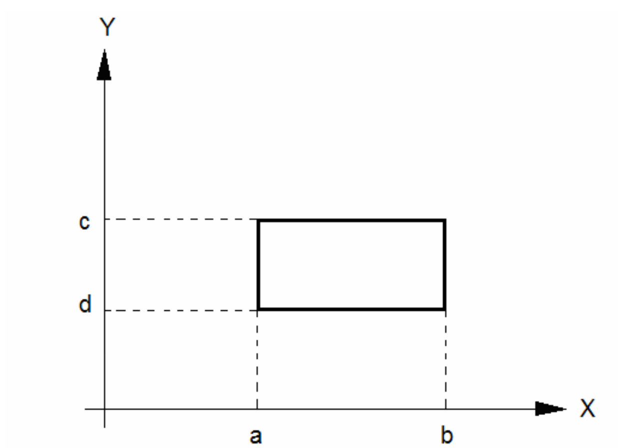

Figure (7): An interval vector

Transformation of Interval to Perturbation

Perturbation methods often use small change in a parameter ε. To express interval problems in terms of perturbation, an interval perturbation, $\varepsilon = [-1,1]$, is introduced so that a general interval is written as summation of center and radial values.

Considering $\widetilde{Z} = [l, u]$ as an interval number, the median and radius can be defined as:

$$Z_C = (\frac{l+u}{2}) \tag{3.16}$$

$$\widetilde{Z}_R = (\varepsilon)(\frac{u-l}{2}) \tag{3.17}$$

So, $\widetilde{Z}$ can be redefined as:

$$\widetilde{Z} = Z_C + \widetilde{Z}_R \tag{3.18}$$

where, the interval number is shown as its median subjected to a perturbation of radius by which, the result encompasses the range of the interval between the extreme values.

<u>Functional Dependency of Interval Operations</u>

Considering $\widetilde{X} = [-2,2]$ and $\widetilde{Y} = [-2,2]$ as two independent interval numbers, the functional dependent interval multiplication results in:

$$\widetilde{X} \times \widetilde{X} = [0,4]$$

In contrast, the functional independent interval multiplication results in:

$$\widetilde{X} \times \widetilde{Y} = [-4,4]$$

Sharpness Considerations in Engineering

In interval operations, the functional dependency of intervals must be considered in order to attain sharper results. In fact, the issue of sharpness and overestimation in interval bounds is the key limitation in the application of interval methods. Naïve implementation of interval arithmetic algorithms (substituting interval operations for their scalar equivalence) will yield bounds that are not useful for engineering design. Therefore, there is a need to develop algorithms to calculate sharp or nearly sharp bounds to the underlying set theoretic interval problems.

For instance, the calculation of exact sharp bounds to the interval system of equations resulting from linear static analysis using the finite element method has been proved to be computationally combinatorial problem. However, even the 2^n combinations of upper and lower bounds do not always yield the bounds.

In problems with narrow intervals associated with truncation errors, the naïve implementation of interval arithmetic will yield acceptable bounds. However, for wider intervals representing uncertainty in parameters, the naïve method will overestimate the bounds by several orders of magnitude.

Successful applications of the interval method in the linear static problem have required the development of new algorithms that are computationally feasible yet still provide nearly sharp bounds (Muhanna and Mullen 2003).

Objective

The goal of this research is to solve an interval structural dynamics problem, i.e., given uncertainty in material or geometric properties expressed as intervals multiplying element stiffness or mass matrices, find the interval bounds on the structure's response.

One approach for solution to the interval system is applying perturbation theories of mathematics to the interval system. Specifically, perturbation theories in eigenvalue problems, needed for structural dynamics, can be used to obtain the bounds on eigenvalues and eigenvectors that will be addressed in the next chapter. However, some perturbation theories require the constraint of smallness of the radial perturbation in comparison with the median value. This smallness must be considered throughout the analysis procedure.

CHAPTER IV

MATRIX PERTURBATION THEORIES

4.1 Perturbation of Eigenvalues

The classical linear eigenvalue problem for a symmetric matrix ($[A]=[A]^T$) is:

$$[A]\{x\}=\lambda\{x\} \tag{4.1}$$

with the solution of real eigenvalues ($\lambda_1 \le \lambda_2 \le ... \le \lambda_n$) and corresponding eigenvectors ($x_1, x_2, ..., x_n$). This equation can be transformed into a ratio of quadratics known as the Rayleigh quotient:

$$R(x)=\frac{\{x\}^T[A]\{x\}}{\{x\}^T\{x\}} \tag{4.2}$$

Transforming the Rayleigh quotient to the principal basis with the orthogonal matrix $[Q]$ (matrix of eigenvectors) obtained by the eigenvalue decomposition of matrix ($[A]=[Q][\Lambda][Q]^T$), in which $[\Lambda]$ is the diagonal matrix of eigenvalues and ($\{y\}=[Q]^T\{x\}$), the quotient becomes:

$$R(x)=\frac{([Q]\{y\})^T[A]([Q]\{y\})}{([Q]\{y\})^T([Q]\{y\})}=\frac{\{y\}^T[\Lambda]\{y\}}{\{y\}^T\{y\}}=\frac{\lambda_1 y_1^2+\lambda_2 y_2^2+...+\lambda_n y_n^2}{y_1^2+...+y_n^2} \tag{4.3}$$

Furthermore:

$$R(x) = \frac{\lambda_1 (y_1^2 + \frac{\lambda_2}{\lambda_1} y_2^2 + ... + \frac{\lambda_n}{\lambda_1} y_n^2)}{y_1^2 + ... + y_n^2} \geq \lambda_1 \tag{4.4}$$

$$R(x) = \frac{\lambda_n (\frac{\lambda_1}{\lambda_n} y_1^2 + \frac{\lambda_2}{\lambda_n} y_2^2 + ... + y_n^2)}{y_1^2 + ... + y_n^2} \leq \lambda_n \tag{4.5}$$

Therefore, the Rayleigh quotient for a symmetric matrix is bounded between the smallest and the largest eigenvalues (Strang 1976).

$$\lambda_1 \leq R(x) = \frac{\{x\}^T [A] \{x\}}{\{x\}^T \{x\}} \leq \lambda_n \tag{4.6}$$

Thus, the first eigenvalue (λ_1) can be obtained by performing an unconstrained minimization on the scalar-valued function of Rayleigh quotient:

$$\min_{x \in R^n} R(x) = \min_{x \in R^n} (\frac{\{x\}^T [A] \{x\}}{\{x\}^T \{x\}}) = \lambda_1 \tag{4.7}$$

In order to find the intermediate eigenvalues, additional constraints must be imposed on this minimization problem. The second eigenvalue can be determined by imposing a single constraint, i.e., the trial vector $\{x\}$ shall be perpendicular to an arbitrary vector $\{z\}$ $(\{x\}^T \{z\} = 0)$.This restriction changes the problem to a set of constrained minimizations whose upper-bound is the second smallest eigenvalue (λ_2). So for any choice of $\{z\}$:

$$\min_{x^T z = 0} R(x) = \mu_1(z) \leq \lambda_2 \tag{4.8}$$

This is proven by considering the trial vector $\{x\}$ as a non-zero combination of the first and second normalized eigenvectors:

$$\{x\} = \alpha\{x_1\} + \beta\{x_2\} \tag{4.9}$$

in which, $\{x\}$ will be orthogonal to $\{z\}$. This only imposes a single condition on (α) and (β). For any combination of the first two eigenvectors:

$$R(x) = \frac{(\alpha\{x_1\} + \beta\{x_2\})^T [A](\alpha\{x_1\} + \beta\{x_2\})}{(\alpha\{x_1\} + \beta\{x_2\})^T (\alpha\{x_1\} + \beta\{x_2\})} = \frac{\lambda_1\alpha^2 + \lambda_2\beta^2}{\alpha^2 + \beta^2} \leq \lambda_2 \tag{4.10}$$

Therefore, the minimization of $R(x)$ subject to a single constraint $(\{x\}^T\{z\} = 0)$ and then choosing the vector $\{z\}$ that maximizes these minima yields the second smallest eigenvalue (λ_2).

$$\lambda_2 = \max[\min_{x^T z=0} R(x)] \tag{4.11}$$

This result can be generalized to obtain the next eigenvalues by applying additional constraints to $R(x)$ as:

$$\lambda_k = \max[\min R(x)] \tag{4.12}$$

(subject to constrains $(\{x\}^T\{z_i\} = 0), i = 1,...k-1, k \geq 2$)

This principle is called the *maximin* characterization of eigenvalues for symmetric matrices.

Geometric Observation

Geometrically, if [A] is positive definite, the numerator of the Rayleigh quotient ($\{x\}^T [A]\{x\} = 1$) defines a hyper-ellipsoid in n-dimensional space which is centered at the origin. Transforming the system to the principal basis, the equation of the hyper-ellipsoid is:

$$\lambda_1 y_1^2 + \lambda_2 y_2^2 + \ldots + \lambda_n y_n^2 = 1 \tag{4.13}$$

Therefore, the principal axes of the hyper-ellipsoid are in the directions of the eigenvectors. Furthermore, pointing to the direction of the jth eigenvector $[(y_i = 0), (i \neq j)]$:

$$\lambda_j y_j^2 = 1 \rightarrow y_j = \frac{1}{\sqrt{\lambda_j}} \tag{4.14}$$

Thus the length of each semi-axis is the reciprocal of the square root of the eigenvalue whose corresponding eigenvector is collinear with that semi-axis (Strang 1976). Therefore, performing the unconstrained minimization on the Rayleigh quotient, which finds the absolute minimum (λ_1), can geometrically be interpreted as determining the semi-axis of greatest length $(y_1 = 1/\sqrt{\lambda_1})$.

Passing an arbitrary plane through the origin of hyper-ellipsoid creates a cross-section which is again an ellipsoid, in one lower dimension. If this cross-sectional ellipsoid is rotated until its greatest semi-axis $(1/\sqrt{\mu_1})$ assumes its smallest value, the semi-axis of the original ellipsoid of second greatest length is determined $(y_2 = 1/\sqrt{\lambda_2})$.

This observation can be considered as the geometric interpretation of the concept of maximin characterization of eigenvalues for symmetric matrices. Figure (8) shows this concept for a 3D ellipsoid schematically.

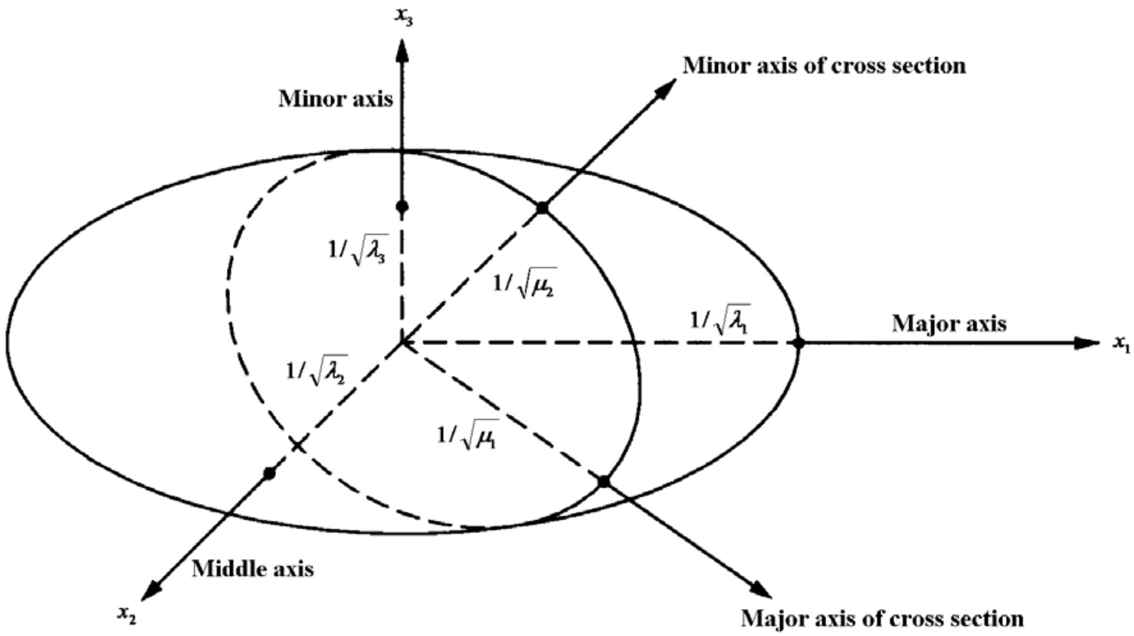

Figure (8): 3D Ellipsoid and its elliptic cross-section

with semi-axes related to eigenvalues

Symmetric Matrix Non-Negative Definite Perturbation

If the symmetric matrix [A] is subjected to a symmetric non-negative definite perturbation matrix $[E]$, $(\{x\}^T[E]\{x\} \geq 0)$ using the unconstrained minimization of $R(x)$, the first eigenvalue of the perturbed matrix is:

$$\hat{\lambda}_1(A+E) = \min \frac{\{x\}^T[A+E]\{x\}}{\{x\}^T\{x\}} \geq \min \frac{\{x\}^T[A]\{x\}}{\{x\}^T\{x\}} = \lambda_1(A) \tag{4.15}$$

For the next eigenvalues of the perturbed matrix, the maximin characterization of eigenvalues can be used as:

$$\hat{\lambda}_k(A+E) = \max[\min_{x^T z_i=0, i=1,\ldots,k-1} \frac{\{x\}^T[A+E]\{x\}}{\{x\}^T\{x\}}] \geq \max[\min_{x^T z_i=0, i=1,\ldots,k-1} \frac{\{x\}^T[A]\{x\}}{\{x\}^T\{x\}}] = \lambda_k(A) \tag{4.16}$$

Therefore, all eigenvalues of a symmetric matrix subject to a non-negative definite perturbation monotonically increase from the eigenvalues of the exact matrix.

$$\hat{\lambda}_k(A+E) \geq \lambda_k(A) \tag{4.17}$$

Similarly, all eigenvalues of a symmetric matrix subject to a non-positive definite perturbation monotonically decrease from the eigenvalues of the exact matrix.

$$\hat{\lambda}_k(A-E) \leq \lambda_k(A) \tag{4.18}$$

This concept is known as the “monotonic behavior” of eigenvalues of symmetric matrices subject to a symmetric non-negative (or non-positive) perturbation (Bellman 1960).

4.2 Perturbation of Eigenvectors

4.2.1 Theory of Simple Invariant Subspaces

Invariant Subspace

The subspace χ is defined to be an *invariant subspace* of matrix $[A]$ if:

$$A\chi \subset \chi \tag{4.19}$$

This means that if χ is an invariant subspace of $[A]_{n\times n}$ and also, columns of $[X_1]_{n\times m}$ form a basis for χ, then there is a unique matrix $[L_1]_{m\times m}$ such that:

$$[A][X_1] = [X_1][L_1] \tag{4.20}$$

The matrix $[L_1]$ is the representation of $[A]$ on χ with respect to the basis $[X_1]$ and the eigenvalues of $[L_1]$ are a subset of eigenvalues of $[A]$. Therefore, for the invariant subspace, $(\{v\},\lambda)$ is an eigenpair of $[L_1]$ if and only if $(\{[X_1]\{v\}\},\lambda)$ is an eigenpair of $[A]$.

Theorem of Invariant Subspaces

For a real symmetric matrix $[A]$, considering the subspace χ with the linearly independent columns of $[X_1]$ forming a basis for χ and the linearly independent columns of $[X_2]$ spanning the complementary subspace $\chi^{\perp}$, then, χ is an invariant subspace of $[A]$ if and only if:

$$[X_2]^T[A][X_1] = [0] \tag{4.21}$$

Therefore, invoking the necessary and sufficient condition and postulating the definition of invariant subspaces, the symmetric matrix $[A]$ can be reduced to a diagonalized form using a unitary similarity transformation as:

$$[X_1 X_2]^T[A][X_1 X_2] = \begin{bmatrix} [X_1]^T[A][X_1] & [X_1]^T[A][X_2] \\ [X_2]^T[A][X_1] & [X_2]^T[A][X_2] \end{bmatrix} = \begin{bmatrix} [L_1] & [0] \\ [0] & [L_2] \end{bmatrix} \tag{4.22}$$

where $[L_i] = [X_i]^T[A][X_i],\ i = 1,2.$

Simple Invariant Subspace

An invariant subspace is *simple* if the eigenvalues of its representation $[L_1]$ are distinct from other eigenvalues of $[A]$. Thus, using the reduced form of $[A]$ with respect to the unitary matrix $[[X_1][X_2]]$, χ is a *simple* invariant subspace if the eigenvalues of $[L_1]$ and $[L_2]$ are distinct:

$$\lambda([L_1]) \cap \lambda([L_2]) = \varnothing \tag{4.23}$$

Spectral Resolution

The symmetric matrix $[A]$ can be decomposed as the summation of contributions of simple invariant subspaces χ and $\chi^{\perp}$ as:

$$[A]=[X_1][L_1][X_1]^T+[X_2][L_2][X_2]^T \tag{4.24}$$

which is the spectral resolution of the matrix $[A]$ into two complementary invariant subspaces.

Spectral Projection

Considering the projection matrices $[P_i]=[X_i][X_i]^T$, $i=1,2$ with properties as:

$$[P_i]^2=[P_i]\ (i=1,2) \tag{4.25a}$$

$$[P_1][P_2]=[P_2][P_1]=[0] \tag{4.25b}$$

$$[A]=[P_1][A][P_1]+[P_2][A][P_2] \tag{4.25c}$$

hence, any vector $\{z\}$ can be decomposed into the sum of two vectors, $\{z\}=\{x_1\}+\{x_2\}$ and ($\{x_1\}\in\chi$, $\{x_2\}\in\chi^{\perp}$), in which, the decomposed component vectors are obtained using projection matrices as:

$$\{x_1\}=[P_1]\{z\} \tag{4.26}$$

$$\{x_2\}=([I]-[P_1])\{z\}=[P_2]\{z\} \tag{4.27}$$

which are known as spectral projections of simple invariant subspaces.

4.2.2 Perturbation of Simple Invariant Subspaces

Considering the column spaces of $[X_1]$ and $[X_2]$ to span two complementary simple invariant subspaces, the perturbed orthogonal subspaces are defined as:

$$[\hat{X}_1] = [X_1] + [X_2][P] \tag{4.28}$$

$$[\hat{X}_2] = [X_2] - [X_1][P]^T \tag{4.29}$$

in which $[P]$ is a matrix to be determined. Thus, each perturbed subspace is defined as a summation of the exact subspace and the contribution of the complementary subspace.

<u>Orthonormalization:</u>

Performing inner products on each perturbed subspace, Eqs(4.28,4.29), as:

$$[\hat{X}_1]^T[\hat{X}_1] = ([I] + [P]^T[P]) \tag{4.30}$$

$$[\hat{X}_2]^T[\hat{X}_2] = ([I] + [P][P]^T) \tag{4.31}$$

the perturbed complementary subspaces can be orthonormalized as:

$$[\hat{X}_1] = ([X_1] + [X_2][P])([I] + [P]^T[P])^{-\frac{1}{2}} \tag{4.32}$$

$$[\hat{X}_2] = ([X_2] - [X_1][P]^T)([I] + [P][P]^T)^{-\frac{1}{2}} \tag{4.33}$$

in which, the redefined perturbed subspaces have orthonormal columns.

Perturbation Problem

Considering a symmetric perturbation $[E]$, the perturbed matrix is defined as:

$$[\hat{A}] = [A] + [E] \tag{4.34}$$

Performing the similarity transformation on the symmetric perturbed matrix $[\widetilde{A}]$ using the unitary matrix $[[\hat{X}_1][\hat{X}_2]]$ obtained from the orthonormalized perturbed subspaces as:

$$[\hat{X}_1 \hat{X}_2]^T [\hat{A}][\hat{X}_1 \hat{X}_2] = \begin{bmatrix} [\hat{L}_1] & [\hat{G}]^T \\ [\hat{G}] & [\hat{L}_2] \end{bmatrix} \tag{4.35}$$

Then, using the theorem of invariant subspaces, $[\hat{X}_1]$ is an invariant subspace if and only if:

$$[\hat{G}] = [\hat{X}_2]^T [\hat{A}][\hat{X}_1] = [0] \tag{4.36}$$

Substituting the perturbed matrix and perturbed subspaces, Eqs.(4.32-4.34), and linearizing the result due to a small perturbation compared to the unperturbed matrix, Eq(4.36) is rewritten as:

$$[P][L_1] - [L_2][P] = [X_2]^T [E][X_1] \tag{4.37}$$

This perturbation problem is an equation for unknown $[P]$ in the form of a Sylvester's equation.

Sylvester's Equation

A Sylvester's equation (J. J. Sylvester 1814-1897) is of the form:

$$[A][X]-[X][B]=[C] \tag{4.38}$$

in which, $[A]_{n\times n}$, $[B]_{m\times m}$ and $[C]_{n\times m}$ are known matrices, and $[X]_{n\times m}$ is the unknown matrix to be determined. Equivalently, a linear operator $[T]$ can be defined as:

$$[T]=[X]_{n\times m}\rightarrow([A][X]-[X][B])_{n\times m} \tag{4.39}$$

The uniqueness of the solution to the Sylvester's equation is guaranteed when the operator $[T]$ is nonsingular. The operator $[T]$ is nonsingular if and only if the eigenvalues of $[A]$ and $[B]$ are distinct:

$$\lambda([A])\cap\lambda([B])=\varnothing \tag{4.40}$$

Thus, for the perturbation problem, Eq.(4.37), the uniqueness of the solution matrix $[P]$ is guaranteed if the eigenvalues of $[L_1]$ and $[L_2]$ are distinct and hence, for the uniqueness, the column spaces of $[X_1]$ and $[X_2]$ must span two simple invariant subspaces, Eq.(4.23).

4.2.3 Perturbation of Eigenvectors

The perturbation of the first eigenvector, using Eq.(4.28), is defined as:

$$\{\hat{x}_1\} = \{x_1\} + [X_2][p] \tag{4.41}$$

Thus, the perturbation problem, Eq.(4.37), is considerably simplified as:

$$[p]\lambda_1 - [L_2][p] = [X_2]^T[E]\{x_1\} \tag{4.42}$$

since, the operator $[T]$ is specialized as $(\lambda_1[I]-[L_2])$. If (λ_1) is a simple eigenvalue, the solution for $[p]$ exists and is unique as:

$$[p] = (\lambda_1[I]-[L_2])^{-1}[X_2]^T[E]\{x_1\} \tag{4.43}$$

Therefore the perturbed eigenvector is:

$$\{\hat{x}_1\} = \{x_1\} + [X_2](\lambda_1[I]-[L_2])^{-1}[X_2]^T[E]\{x_1\} \tag{4.44}$$

Also, the number $\left\| [X_2](\lambda_1[I]-[L_2])^{-1}[X_2]^T \right\|$ is known as the condition number of the eigenvector $\{x_1\}$ (Stewart and Guang 1991).

For each eigenvalue, the perturbed eigenvector can be found using Eq. (4.44).

CHAPTER V

INTERVAL RESPONSE SPECTRUM ANALYSIS

As mentioned in chapter II, in the presence of uncertainty in the structure's geometrical or material characteristics, the conventional response spectrum analysis cannot be performed to obtain the structure's responses. In this work, a new method is developed which is capable of performing a response spectrum analysis and obtaining the bounds on the structure's response when the parameters in the structure are unknown but bounded. This method, entitled Interval Response Spectrum Analysis (IRSA), enhances the procedure in deterministic response spectrum analysis to take into account the existence of interval uncertainty throughout the solution process.

5.1 IRSA Procedure:

First, IRSA defines the uncertainty in the system's parameters as closed intervals, therefore, the imprecise property can vary within the intervals between extreme values (bounds). Then, having the uncertain parameters represented by interval variables for each element, the interval global stiffness and mass matrices of MDOF system are assembled. This assemblage is performed such that the element physical characteristics and the matrix mathematical properties are preserved.

Then an interval generalized eigenvalue problem between the interval stiffness and mass matrices is established. From this interval eigenvalue problem, two solutions of interest are obtained:

1. Bounds on variation of circular natural frequencies (Interval natural frequencies)
2. Bounds on directional deviation of mode shapes (Interval mode shapes)

Then, the interval modal coordinate and the maximum modal coordinate are determined using the excitation response spectrum evaluated for the corresponding interval of natural circular frequency and assumed modal damping ratio. Then, the interval modal participation factor is computed. Dependency or independency of variations in interval modal participation factor is considered. Following this, the maximum modal response is computed as a maximum of the product of the maximum modal coordinate, the interval modal participation factor and the interval mode shape. Finally, the contributions of all maximum modal responses are combined to determine the maximum total response using SRSS or other combination methods.

5.2 Interval Representation of Uncertainty

The presence of uncertainty in a structure's physical or geometrical property can be depicted by a closed interval. Considering $\tilde{q}$ as a structure's uncertain parameter:

$$\tilde{q} = [l, u] \tag{5.1}$$

in which, l and u are the lower and upper bounds of the uncertain parameter, respectively.

5.2.1 Interval Stiffness Matrix

The structure's deterministic global stiffness matrix can be viewed as a linear summation of the element contributions to the global stiffness matrix,

$$[K] = \sum_{i=1}^{n} [L_i][K_i][L_i]^T \tag{5.2}$$

where, $[L_i]$ is the element Boolean connectivity matrix and $[K_i]$ is the element stiffness matrix in the global coordinate system (a geometric second-order tensor transformation may be required from the element local coordinates to the structure's global coordinates). Considering the presence of uncertainty in the stiffness characteristics, the non-deterministic element stiffness matrix is expressed as:

$$[\widetilde{K}_i] = ([l_i, u_i])[K_i] \tag{5.3}$$

in which $[l_i, u_i]$ is an interval number that pre-multiplies the deterministic element stiffness matrix.

Considering the variation as a multiplier outside of the stiffness matrix preserves the element physical characteristics such as real natural frequencies and rigid body modes as well as stiffness matrix properties such as symmetry and positive semi-definiteness. In terms of the physics of the system, this means that the stiffness within each element is unknown but bounded and has a unique value that can independently vary from the stiffness of other elements.

This parametric form must be used to preserve sharp interval bounds. The uncertainty in each element's stiffness is assumed to be independent. For a substructure with an overall interval uncertainty, Eqs.(5.2,5.3) are used to assemble the substructure's stiffness matrix.

For coupled elements, matrix decompositions can be used. For instance, in a beam-column, if functional independent values of axial and bending properties are uncertain, the axial and bending components can be additively decomposed as:

$$[\widetilde{K}_i] = ([l_i, u_i]_{Axial})[K_i]_{Axial} + ([l_i, u_i]_{Bending})[K_i]_{Bending} \tag{5.4}$$

Likewise, for continuum problems with functional independent uncertain properties at integration points, the contribution of each integration point can be assembled independently.

Interval Global Stiffness Matrix

The structure's global stiffness matrix in the presence of any uncertainty is the linear summation of the contributions of non-deterministic interval element stiffness matrices:

$$[\widetilde{K}] = \sum_{i=1}^{n} [L_i]\{([l_i, u_i])[K_i]\}[L_i]^T \tag{5.5}$$

or:

$$[\widetilde{K}] = \sum_{i=1}^{n} ([l_i, u_i])[L_i][K_i][L_i]^T = \sum_{i=1}^{n} ([l_i, u_i])[\overline{K}_i] \tag{5.6}$$

in which $[\overline{K}_i]$ is the deterministic element stiffness contribution to the global stiffness matrix.

5.2.2 Interval Mass Matrix

Similarly, the structure's deterministic global mass matrix is viewed as a linear summation of the element contributions to the global mass matrix as:

$$[M] = \sum_{i=1}^{n} [L_i][M_i][L_i]^T \tag{5.7}$$

where, $[M_i]$ is the element stiffness matrix in the global coordinate system.

Considering the presence of uncertainty in the mass properties, the non-deterministic element mass matrix is:

$$[\widetilde{M}_i] = ([l_i, u_i])[M_i] \tag{5.8}$$

in which $[l_i, u_i]$ is an interval number that pre-multiplies the deterministic element mass matrix. Considering the variation as a multiplier outside of the mass matrix preserves the element physical properties. Analogous to the interval stiffness matrix, this procedure preserves the physical and mathematical characteristics of the mass matrix.

The structure's global mass matrix in the presence of any uncertainty is the linear summation of the contributions of non-deterministic interval element mass matrices:

$$[\widetilde{M}] = \sum_{i=1}^{n} [L_i]\{([l_i, u_i])[M_i]\}[L_i]^T \tag{5.9}$$

or:

$$[\widetilde{M}] = \sum_{i=1}^{n} ([l_i, u_i])[L_i][M_i][L_i]^T = \sum_{i=1}^{n} ([l_i, u_i])[\overline{M}_i] \tag{5.10}$$

in which $[\overline{M}_i]$ is the deterministic element mass contribution to the global mass matrix.

CHAPTER VI

BOUNDS ON NATURAL FREQUENCIES AND MODE SHAPES

6.1 Interval Eigenvalue Problem

The eigenvalue problems for matrices containing interval values are known as the interval eigenvalue problems. Therefore, if $[\widetilde{A}]$ is an interval real matrix $(\widetilde{A} \in \Re^{n \times n})$ and $[A]$ is a member of the interval matrix $(A \in \widetilde{A})$ or in terms of components $(a_{ij} \in \widetilde{a}_{ij})$, the interval eigenvalue problem is shown as:

$$([A] - \lambda[I])\{x\} = 0, (A \in \widetilde{A}) \tag{6.1}$$

6.1.1 Solution for Eigenvalues

The solution of interest to the real interval eigenvalue problem for bounds on each eigenvalue is defined as an inclusive set of real values $(\widetilde{\lambda})$ such that for any member of the interval matrix, the eigenvalue solution to the problem is a member of the solution set. Therefore, the solution to the interval eigenvalue problem for each eigenvalue can be mathematically expressed as:

$$\{\lambda \in \widetilde{\lambda} = [\lambda^l, \lambda^u] \mid \forall A \in \widetilde{A} : ([A] - \lambda[I])\{x\} = 0\} \tag{6.2}$$

6.1.2 Solution for Eigenvectors

The solution of interest to the real interval eigenvalue problem for bounds on each eigenvector is defined as an inclusive set of real values of vector $\{\widetilde{x}\}$ such that for any member of the interval matrix, the eigenvector solution to the problem is a member of the solution set. Thus, the solution to the interval eigenvalue problem for each eigenvector is:

$$\{\{x\} \in \{\widetilde{x}\} \mid \forall A \in \widetilde{A}, \lambda : ([A] - \lambda[I])\{x\} = 0\} \tag{6.3}$$

6.2 Interval Eigenvalue Problem for Structural Dynamics

For dynamics problems, the interval generalized eigenvalue problem between the interval stiffness and mass matrices can be set up by substituting the interval global stiffness and mass matrices, Eq.(5.6,5.10), into Eq.(2.11). Therefore, the non-deterministic interval eigenvalue problem is obtained as:

$$(\sum_{i=1}^{n}([l_i, u_i])[\overline{K}_i])\{\widetilde{\varphi}\} = (\widetilde{\omega}^2)\sum_{i=1}^{n}([l_i, u_i])[\overline{M}_i])\{\widetilde{\varphi}\} \tag{6.4}$$

Hence, determination of bounds on natural frequencies in the presence of uncertainty can be mathematically interpreted as performing an interval eigenvalue problem on the interval-set-represented non-deterministic stiffness and mass matrices. Two solutions of interest are:

$(\widetilde{\omega})$: Interval natural frequencies or bounds on variation of circular natural frequencies.

$\{\widetilde{\varphi}\}$: Interval mode shapes or bounds on directional deviation of mode shapes.

While the element mass matrix contribution can also have interval uncertainty, in this work only problems with interval stiffness properties are addressed. However, for functional independent variations for both mass and stiffness matrices, the extension of the proposed work is straightforward.

6.2.1 Transformation of Interval to Perturbation in Eigenvalue Problem

The interval eigenvalue problem for a structure's with stiffness properties expressed as interval values is:

$$(\sum_{i=1}^{n}([l_i,u_i])[\overline{K}_i])\{\tilde{\varphi}\} = (\tilde{\omega}^2)\sum_{i=1}^{n}([M)\{\tilde{\varphi}\} \tag{6.5}$$

This interval eigenvalue problem can be transformed to a pseudo-deterministic eigenvalue problem subjected to a matrix perturbation. Introducing the central and radial (perturbation) stiffness matrices as:

$$[K_C] = \sum_{i=1}^{n}(\frac{l_i+u_i}{2})[\overline{K}_i] \tag{6.6}$$

$$[\tilde{K}_R] = \sum_{i=1}^{n}(\varepsilon_i)(\frac{u_i-l_i}{2})[\overline{K}_i] \quad , \quad \varepsilon_i = [-1,1] \tag{6.7}$$

Using Eqs. (6.6,6.7), the non-deterministic interval eigenpair problem, Eq.(6.5), becomes:

$$([K_C]+[\tilde{K}_R])\{\tilde{\varphi}\} = (\tilde{\omega}^2)[M]\{\tilde{\varphi}\} \tag{6.8}$$

Hence, the determination of bounds on natural frequencies and bounds on mode shapes of a system in the presence of uncertainty in the stiffness properties is mathematically interpreted as an eigenvalue problem on a central stiffness matrix ($[K_C]$) that is subjected to a radial perturbation stiffness matrix ($[\widetilde{K}_R]$). This perturbation is in fact, a linear summation of non-negative definite deterministic element stiffness contribution matrices that are scaled with bounded real numbers (ε_i).

6.3 Bounding the Natural Frequencies

6.3.1 Eigenvalue Perturbation Considerations

A real symmetric matrix subjected to an arbitrary perturbation can produce complex conjugate eigenvalues and therefore, the bounds on eigenvalues are then in the complex domain. However, since the stiffness and mass matrices governing the structural behavior are symmetric, the natural frequencies of the structure are always real. To retain correct physical results, constraints must be imposed on the non-deterministic eigenvalue problem. These constraints are intrinsically present in the non-deterministic eigenpair problem. These constraints result in a radial perturbation matrix ($[\widetilde{K}_R]$) which is a linear combination of non-negative definite matrices that are scaled by bounded real numbers. Therefore, this characteristic of the radial perturbation matrix must be considered in the development of any scheme to bound the natural frequencies.

6.3.2 Determination of Eigenvalue Bounds (Interval Natural Frequencies)

Using the concepts of minimum and maximin characterizations of eigenvalues for symmetric matrices, Eqs.(4.7,4.12), the solution to the generalized interval eigenvalue problem for the vibration of a structure with uncertainty in the stiffness characteristics, Eq.(6.8), is shown as:

For the first eigenvalue:

$$\widetilde{\lambda}_1(K_C + \widetilde{K}_R) = \min_{x \in R^n}\left(\frac{\{x\}^T[K_C + \widetilde{K}_R]\{x\}}{\{x\}^T[M]\{x\}}\right) = \min_{x \in R^n}\left(\frac{\{x\}^T[K_C]\{x\}}{\{x\}^T[M]\{x\}} + \frac{\{x\}^T[\widetilde{K}_R]\{x\}}{\{x\}^T[M]\{x\}}\right) \tag{6.9}$$

For the next eigenvalues:

$$\begin{aligned} \widetilde{\lambda}_k(K_C + \widetilde{K}_R) &= \max\Big[\min_{x^T z_i = 0, i=1,\dots,k-1} \frac{\{x\}^T[K_C + \widetilde{K}_R]\{x\}}{\{x\}^T[M]\{x\}}\Big] = \\ &\max\Big[\min_{x^T z_i = 0, i=1,\dots,k-1}\Big(\frac{\{x\}^T[K_C]\{x\}}{\{x\}^T[M]\{x\}} + \frac{\{x\}^T[\widetilde{K}_R]\{x\}}{\{x\}^T[M]\{x\}}\Big)\Big] \end{aligned} \tag{6.10}$$

Substituting and expanding the right-hand side terms of Eqs. (6.9,6.10):

$$\begin{aligned} &\left(\frac{\{x\}^T[K_C]\{x\}}{\{x\}^T[M]\{x\}} + \frac{\{x\}^T[\widetilde{K}_R]\{x\}}{\{x\}^T[M]\{x\}}\right) = \\ &\sum_{i=1}^{n}\left(\frac{l_i + u_i}{2}\right)\left(\frac{\{x\}^T[\overline{K}_i]\{x\}}{\{x\}^T[M]\{x\}}\right) + \sum_{i=1}^{n}(\varepsilon_i)\left(\frac{u_i - l_i}{2}\right)\left(\frac{\{x\}^T[\overline{K}_i]\{x\}}{\{x\}^T[M]\{x\}}\right) \end{aligned} \tag{6.11}$$

Since the matrix $[\overline{K}_i]$ is non-negative definite, the term $(\frac{\{x\}^T[\overline{K}_i]\{x\}}{\{x\}^T[M]\{x\}})$ is non-negative. Therefore, based on the monotonic behavior of eigenvalues for symmetric matrices, Eqs.(4.17,4.18) the upper bounds on the eigenvalues in Eqs.(6.9,6.10) are obtained by considering maximum values of interval coefficients of uncertainty $(\varepsilon_i = [-1,1])$, $((\varepsilon_i)_{\max} = 1)$, for all elements in the radial perturbation matrix. Similarly, the lower bounds on the eigenvalues are obtained by considering minimum values of those coefficients, $((\varepsilon_i)_{\min} = -1)$, for all elements in the radial perturbation matrix. Also, it can be observed that any other element stiffness selected from the interval set will yield eigenvalues between the upper and lower bounds.

Hence, the bounds on the eigenvalues of the perturbed matrix are obtained as:

$$\max[\widetilde{\lambda}_k(K_C + \widetilde{K}_R)] = \lambda_k(\sum_{i=1}^{n}(\frac{l_i + u_i}{2})[\overline{K}_i] + \sum_{i=1}^{n}((\varepsilon_i)_{\max})(\frac{u_i - l_i}{2})[\overline{K}_i])) = \lambda_k(\sum_{i=1}^{n}(u_i)[\overline{K}_i]) \tag{6.12}$$

$$\min[\widetilde{\lambda}_k(K_C + \widetilde{K}_R)] = \lambda_k(\sum_{i=1}^{n}(\frac{l_i + u_i}{2})[\overline{K}_i] + \sum_{i=1}^{n}((\varepsilon_i)_{\min})(\frac{u_i - l_i}{2})[\overline{K}_i])) = \lambda_k(\sum_{i=1}^{n}(l_i)[\overline{K}_i]) \tag{6.13}$$

Therefore, the deterministic eigenvalue problems corresponding to the maximum and minimum natural frequencies are obtained as:

$$(\sum_{i=1}^{n}(u_i)[\overline{K}_i])\{\varphi\} = (\omega_{\max}^2)[M]\{\varphi\} \tag{6.14}$$

$$(\sum_{i=1}^{n}(l_i)[\overline{K}_i])\{\varphi\} = (\omega_{\min}^2)[M]\{\varphi\} \tag{6.15}$$

This means that in the presence of any interval uncertainty in the stiffness of structural elements, the exact upper bounds of natural frequencies are obtained by using the upper values of stiffness for all elements in a deterministic generalized eigenvalue problem. Similarly, the exact lower bounds of natural frequencies are obtained by using the lower values of stiffness for all elements in another deterministic generalized eigenvalue problem.

6.4 Bounding the Mode Shapes

6.4.1 Determination of Eigenvector Bounds (Interval Mode Shapes)

The perturbed generalized eigenvalue problem for structural dynamics, Eq.(6.8) can be transformed to a perturbed classic eigenpair problem as:

$$([M]^{-\frac{1}{2}}[K_C][M]^{-\frac{1}{2}} + [M]^{-\frac{1}{2}}[\widetilde{K}_R][M]^{-\frac{1}{2}})\{\widetilde{\varphi}\} = (\widetilde{\omega}^2)\{\widetilde{\varphi}\} \tag{6.16}$$

hence, the symmetric perturbation matrix is:

$$[E] = [M]^{-\frac{1}{2}}[\widetilde{K}_R][M]^{-\frac{1}{2}} \tag{6.17}$$

Substituting for radial stiffness $[\widetilde{K}_R]$, Eq.(6.7), in Eq.(6.17), the error matrix becomes:

$$[E] = [M]^{-\frac{1}{2}}(\sum_{i=1}^{n}(\varepsilon_i)(\frac{u_i - l_i}{2})[\overline{K}_i])[M]^{-\frac{1}{2}} \tag{6.18}$$

Using the obtained error matrix in eigenvector perturbation equation for the first eigenvector, Eq.(4.44) yield the dynamic perturbed mode shape as:

$$\{\widetilde{\varphi}_1\} = \{\varphi_1\} + ([\Phi_2](\omega_1[I] - [\Omega_2])^{-1}[\Phi_2]^T)([M]^{-\frac{1}{2}}(\sum_{i=1}^{n}(\varepsilon_i)(\frac{u_i - l_i}{2})[\overline{K}_i])[M]^{-\frac{1}{2}})\{\varphi_1\} \tag{6.19}$$

in which, $\{\varphi_1\}$ is the first mode shape, (ω_1) is the first natural circular frequency, $[\Phi_2]$ is the matrix of remaining mode shapes and $[\Omega_2]$ is the diagonal matrix of remaining natural circular frequencies obtained from the unperturbed eigenvalue problem.

Moreover, Eq.(6.19) can be written as:

$$\{\widetilde{\varphi}_1\} = \{\varphi_1\} + [C_1](\sum_{i=1}^{n}(\varepsilon_i)[E_i])\{\varphi_1\} \tag{6.20}$$

in which: $[C_1] = [\Phi_2](\omega_1[I] - [\Omega_2])^{-1}[\Phi_2]^T$ and $[E_i] = (\frac{u_i - l_i}{2})[M]^{-\frac{1}{2}}[\overline{K}_i][M]^{-\frac{1}{2}}, i = 1,...,n$.

Simplifying Eq.(6.20),the interval mode shape is:

$$\{\widetilde{\varphi}_1\} = ([I] + [C_1](\sum_{i=1}^{n}(\varepsilon_i)[E_i]))\{\varphi_1\} \tag{6.21}$$

For the other mode shapes, the same procedure can be used.

CHAPTERVII

BOUNDING DYNAMIC RESPONSE

7.1 Maximum Modal Coordinate

The interval modal coordinate $\widetilde{D}_n$ is determined using the excitation response spectrum evaluated for the corresponding interval of natural circular frequency $\widetilde{\omega}_n$ and assumed modal damping ratio (Figure (9)).

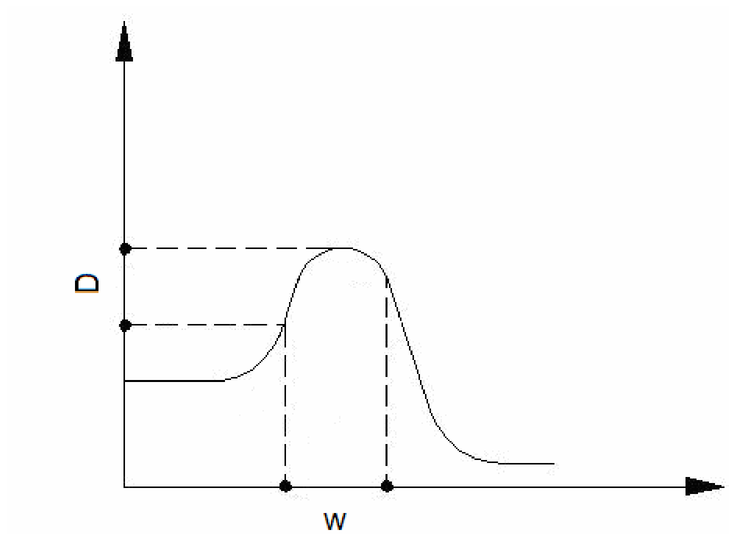

Figure (9): Determination of $\widetilde{D}_n$ corresponding to a $\widetilde{\omega}_n$ for a generic response spectrum

Having the interval modal coordinate, the maximum (upperbound) modal coordinate $D_{n,\max}$ is determined as:

$$D_{n,\max} = \max(\widetilde{D}_n) \tag{7.1}$$

7.2 Interval Modal Participation Factor

If excitation is proportional, the interval modal participation factor is obtained as:

$$\widetilde{\Gamma}_n = \frac{\{\widetilde{\varphi}_n\}^T\{P\}}{M_n} = \frac{\{\widetilde{\varphi}_n\}^T\{P\}}{\{\widetilde{\varphi}_n\}^T[M]\{\widetilde{\varphi}_n\}} \tag{7.2}$$

7.3 Maximum Modal Response

The maximum modal response is determined as the maximum of the product of the maximum modal coordinate, the interval modal participation factor and the interval mode shape as:

$$\{U_{n,\max}\} = \max\big((D_{n,\max})(\widetilde{\Gamma}_n)\{\widetilde{\varphi}_n\}\big) \tag{7.3}$$

To achieve sharper results, functional dependency of intervals in the multiplicative terms must be considered. Maximum modal response, Eq.(7.3), is expanded using the definitions of the interval mode shapes and the interval modal participation factor, Eqs.(6.21,7.2) as:

$$\{U_{n,\max}\} = \max[(D_{n,\max})\frac{\{P\}^T\{\varphi_n\}[I] + (\sum_{i=1}^{N}(\varepsilon_i)(\{P\}^T\{\varphi_n\})[C_n][E_i] +}{\{\varphi_n\}^T[M]\{\varphi_n\} + \{\varphi_n\}^T(\sum_{i=1}^{N}(\varepsilon_i)[M][C_n][E_i])\{\varphi_n\} +}\cdots$$

$$\frac{(\sum_{i=1}^{N}(\varepsilon_i)(\{P\}^T[C_n][E_i]\{\varphi_n\})[I] + (\sum_{i=1}^{N}\sum_{j=1}^{N}(\varepsilon_i)(\varepsilon_j)(\{P\}^T[C_n][E_i]\{\varphi_n\})[C_n][E_i]}{\{\varphi_n\}^T(\sum_{i=1}^{N}(\varepsilon_i)[C_n][E_i][M])\{\varphi_n\} + \{\varphi_n\}^T(\sum_{i=1}^{N}\sum_{j=1}^{N}(\varepsilon_i)(\varepsilon_j)[C_n][E_i][M][C_n][E_j])\{\varphi_n\}}\{\varphi_n\}] \tag{7.4}$$

Thus, considering the dependency of the intervals of uncertainty for each element, (ε_i), the sharper results for maximum modal response are obtained.

7.4 Maximum Total Responses

Finally, the contributions of all maximum modal responses are combined to determine the maximum total response using SRSS or other combination methods.

$$\{U_{\max}\} = \sqrt{\sum_{n=1}^{N} \{U_{n,\max}^2\}} \tag{7.5}$$

7.5 Summary

The interval response spectrum analysis (IRSA) is summarized as following:

1. Define the uncertain physical or geometrical characteristics with closed intervals.

- Determine the interval stiffness matrix $[\tilde{K}]$ and interval mass matrix $[\tilde{M}]$.
- Assume the modal damping ratio ζ_n.

2. Perform an interval eigenvalue problem between the interval stiffness and interval mass matrices.

- Determine the bounds on natural circular frequencies $\tilde{\omega}_n$ (interval natural frequencies).
- Determine the bounds on mode shapes $\{\tilde{\varphi}_n\}$ (interval mode shapes).

3. Compute the maximum modal response.

- Determine the interval modal coordinate $\tilde{D}_n$ and the maximum modal coordinate $D_{n,\max}$ using the excitation response spectrum for the bounds of corresponding natural circular frequency and assumed modal damping ratio.
- Determine the interval modal participation factor $\tilde{\Gamma}_n$.
- Compute the maximum modal response as the product of the maximum modal coordinate, the interval modal participation factor and the interval mode shape.

4. Combine the contributions of all maximum modal responses to determine the maximum total reponse using SRSS or other combination methods.

CHAPTER VIII

NUMERICAL EXAMPLES AND BEHAVIOR OF IRSA METHOD

In this section, the numerical behavior of the IRSA algorithm will be investigated. The computational complexity associated with the behavior will be explored as well as overestimation of interval bounds introduced by the algorithm.

The loss of sharpness as a function of initial interval width will be studied from several example problems.

In addition, the effect of problem size on the interval estimation will be explored and each step in the three step IRSA method (bounds on natural frequencies, mode shapes and response) will be studied.

8.1 Examples for Bounds on Natural Frequencies

The first step in IRSA method is the construction of interval bounds on the natural frequencies of a structure or a finite element mesh. The following problems obtains the bounds on natural frequencies for different systems.

Problem 8.1.1

As the first problem, the bounds on the natural frequencies for a 2D three-element truss with interval uncertainty present in the modulus of elasticity of each element are determined (Figure (10)).

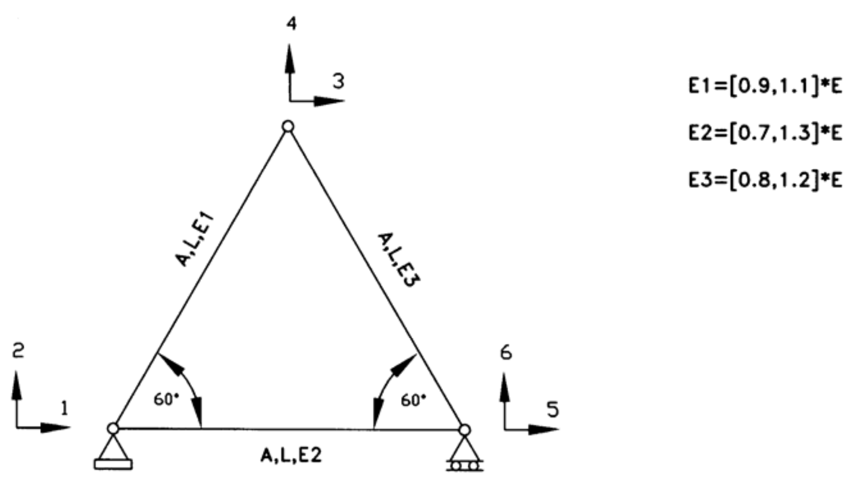

Figure (10): Equilateral truss with material uncertainty

Using the structural stiffness, the lumped mass matrices and the intervals of material uncertainty as:

$$\begin{aligned}
\widetilde{E}_1 &= [E_1^L, E_1^U] = ([0.9,1.1])E \\
\widetilde{E}_2 &= [E_2^L, E_2^U] = ([0.7,1.3])E \\
\widetilde{E}_3 &= [E_3^L, E_3^U] = ([0.8,1.2])E
\end{aligned}$$

the deterministic eigenvalue problems for maximum and minimum natural frequencies, Eqs.(6.14) and (6.15), become:

$$\left(\frac{A}{4L}\begin{bmatrix} E_1^U+E_3^U & \sqrt{3}E_1^U-\sqrt{3}E_3^U & -E_3^U \\ \sqrt{3}E_1^U-\sqrt{3}E_3^U & 3E_1^U+3E_3^U & \sqrt{3}E_3^U \\ -E_3^U & \sqrt{3}E_3^U & 4E_2^U+E_3^U \end{bmatrix} - (\omega_{\max}^2)\rho AL\begin{bmatrix}1&0&0\\0&1&0\\0&0&1\end{bmatrix}\right)\begin{Bmatrix}u_3\\u_4\\u_5\end{Bmatrix}=\{\underline{0}\}$$

$$\left(\frac{A}{4L}\begin{bmatrix} E_1^L+E_3^L & \sqrt{3}E_1^L-\sqrt{3}E_3^L & -E_3^L \\ \sqrt{3}E_1^L-\sqrt{3}E_3^L & 3E_1^L+3E_3^L & \sqrt{3}E_3^L \\ -E_3^L & \sqrt{3}E_3^L & 4E_2^L+E_3^L \end{bmatrix} - (\omega_{\min}^2)\rho AL\begin{bmatrix}1&0&0\\0&1&0\\0&0&1\end{bmatrix}\right)\begin{Bmatrix}u_3\\u_4\\u_5\end{Bmatrix}=\{\underline{0}\}$$

The eigenvalue problems are solved using MATLAB (which uses the transformation to Hessenberg form then finds the eigenvalues and eigenvectors by QR method) The results are summarized in Table (1).

	Lower Bound (L)	Upper Bound (U)	Central Values $(C=\frac{L+U}{2})$	Radial Values $(R=U-C)$	Relative Uncertainty $(\frac{R}{C})$
$\frac{\omega_1 L}{\sqrt{E/\rho}}$	0.5661	0.6964	0.6313	0.0651	0.1032
$\frac{\omega_2 L}{\sqrt{E/\rho}}$	0.8910	1.0936	0.9923	0.1013	0.1021
$\frac{\omega_3 L}{\sqrt{E/\rho}}$	1.2188	1.4897	1.3543	0.1354	0.1000

Table (1): Bounds and central values on non-dimensional frequencies for problem 8.1.1

For comparison, this problem is solved using the combinatorial analysis (lower and upper values of uncertainty for each element), i.e., solving ($2^n = 2^3 = 8$) possible limit state deterministic problems. The results are shown in Table (2):

	E_1=L E_2=L E_3=L	E_1=L E_2=L E_3=U	E_1=L E_2=U E_3=L	E_1=L E_2=U E_3=U	E_1=U E_2=L E_3=L	E_1=U E_2=L E_3=U	E_1=U E_2=U E_3=L	E_1=U E_2=U E_3=U
$\frac{\omega_1 L}{\sqrt{E/\rho}}$	**0.5661**	0.6049	0.6128	0.6685	0.5766	0.6176	0.6310	**0.6964**
$\frac{\omega_2 L}{\sqrt{E/\rho}}$	**0.8910**	0.8956	1.0289	1.0433	0.9326	0.9487	1.0899	**1.0936**
$\frac{\omega_3 L}{\sqrt{E/\rho}}$	**1.2188**	1.3900	1.3289	1.4713	1.2641	1.4208	1.3468	**1.4897**

Table (2): Combination solution for problem 8.1.1

The results obtained by a brute force combination solution yields the same bounds as those obtained by the bounding method of the present work. While all combinations of endpoints do not necessarily provide the extreme values to a general interval problem, based on the results proved in section 6.2.3, this problem is expected to all be bounded by the all lower and all upper values of stiffness.

Problem 8.2.2

The second example problem solves the problem cited in the paper by Qiu, Chen and Elishakoff (1995) using the exact bounding method of the present work. The structure in the problem is a spring-mass system with fixed supports at both ends with interval uncertainty in the elements' stiffness (Figure (11)).

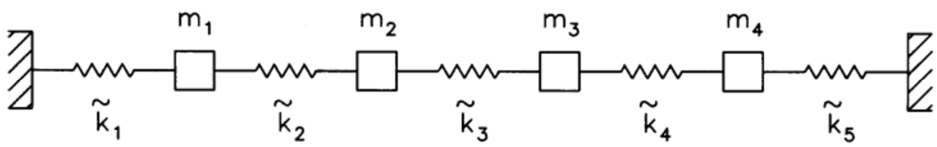

Figure (11): The system of multi-DOF spring-mass system

The central and radial stiffness and central mass matrices given in their work are as following:

$$K^c = 1000 \times \begin{bmatrix} +3 & -2 & 0 & 0 \\ -2 & +5 & -3 & 0 \\ 0 & -3 & +7 & -4 \\ 0 & 0 & -4 & +9 \end{bmatrix} (\frac{N}{m}) \quad , \quad \Delta K = \begin{bmatrix} +25 & -15 & 0 & 0 \\ -15 & +35 & -20 & 0 \\ 0 & -20 & +45 & -25 \\ 0 & 0 & -25 & +55 \end{bmatrix} (\frac{N}{m})$$

$$M^c = diag(1,1,1,1) \ (Kg)$$

Having the problem input information, the individual element interval stiffness matrices (N/m) are back-calculated as:

$$\tilde{K}_1 = ([990,1010])\begin{bmatrix} +1 & -1 \\ -1 & +1 \end{bmatrix} \qquad \tilde{K}_2 = ([1985,2015])\begin{bmatrix} +1 & -1 \\ -1 & +1 \end{bmatrix}$$

$$\tilde{K}_3 = ([2980,3020])\begin{bmatrix} +1 & -1 \\ -1 & +1 \end{bmatrix} \qquad \tilde{K}_4 = ([3975,4025])\begin{bmatrix} +1 & -1 \\ -1 & +1 \end{bmatrix}$$

$$\tilde{K}_5 = ([4970,5030])\begin{bmatrix} +1 & -1 \\ -1 & +1 \end{bmatrix}$$

The eigenvalue problem is solved using the method presented in this work and the results for eigevalues $(1/\sec^2)$ are summarized in Table (3).

	Lower Bound	Upper Bound	Central Values	Radial Values	Relative Uncertainty
$\tilde{\lambda}_1$	898.20	912.12	905.16	6.96	0.00769
$\tilde{\lambda}_2$	3364.86	3414.84	3389.85	24.99	0.00737
$\tilde{\lambda}_3$	7016.10	7112.82	7064.46	48.36	0.00684
$\tilde{\lambda}_4$	12560.84	12720.23	12640.53	79.69	0.00630

Table (3): Solution of the example problem 8.1.2 using the present method

Comparison

The results obtained for problem 8.1.2, using the present method, are compared with the results obtained by Qiu, Chen and Elishakoff (1995) and also with the results obtained by using Dief's method also presented in their paper; Tables (4,5) .

	Lower Bound	Upper Bound	Central Values	Radial Values	Relative Uncertainty
$\tilde{\lambda}_1$	826.74	983.59	905.16	78.42	0.08664
$\tilde{\lambda}_2$	3331.16	3448.53	3389.85	58.69	0.01731
$\tilde{\lambda}_3$	7000.19	7128.72	7064.46	64.26	0.00910
$\tilde{\lambda}_4$	12588.29	12692.77	12640.53	52.24	0.00413

Table (4): Results for problem 8.1.2 by Qiu, Chen and Elishakoff's method

	Lower Bound	Upper Bound	Central Values	Radial Values	Relative Uncertainty
$\tilde{\lambda}_1$	842.93	967.11	905.02	62.09	0.06860
$\tilde{\lambda}_2$	3364.69	3415.01	3389.85	25.16	0.00742
$\tilde{\lambda}_3$	7031.49	7097.54	7064.52	33.02	0.00467
$\tilde{\lambda}_4$	12560.84	12720.23	12640.53	79.69	0.00630

Table (5): Results for problem 8.1.2 by Dief's method

Discussion

The results by Qiu, Chen and Elishakoff (1995) are wider than the present results for lower eigenvalues, however, for higher eigenvalues, their method does not include the whole range of uncertainty. This underestimation is perhaps due to the usage the non-perturbed eigenvectors to obtain the bounds on eigenvalues.

Using Dief's method, the lower eigenvalues have a wider range of uncertainty than the present exact results. At high frequencies, Dief's method provides better bounds. However, all of the bounds provided by Dief's method contain the correct values.

Problem 8.1.3

The third example problem solves a problem cited in the paper by Qiu, Chen and Elishakoff (1996) using the exact bounding method of the present work. The structure in the problem is a 2-D truss with 15 elements and 8 nodes and therefore 13 degrees of active freedom (Figure (12)).

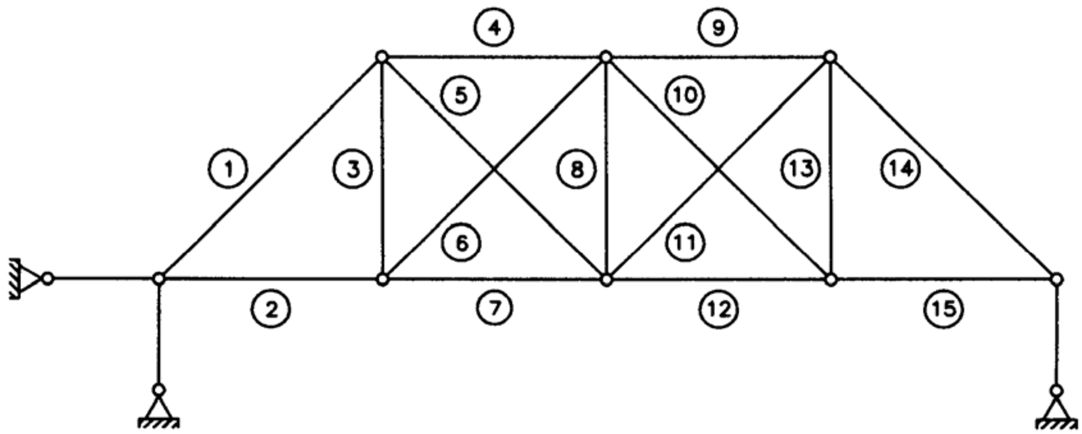

Figure (12): The structure of 2-D truss from Qiu, Chen and Elishakoff (1996)

The cross-sectional area $A = (0.12 \times 10^{-2})m^2$, mass density $\rho = (7800)kg/m^3$, the length for horizontal and vertical members $L = (1)m$, the Young's moduli E of elements 1, 2, 7, 12, 14 and 15 are $\widetilde{E} = [0.205 \times 10^{12}, 0.21 \times 10^{12}]kg/m^2$ and the Young's moduli E of remaining elements are $E = (0.21 \times 10^{12})kg/m^2$.The eigenvalue problem is solved using the method presented in this work and the results are summarized in Table (6).

	Lower Bound	Upper Bound	Central Values	Radial Values	Relative Uncertainty
$\tilde{\lambda}_1$	410329.55	418099.26	414214.41	3884.86	0.00937
$\tilde{\lambda}_2$	1592958.89	1621645.84	1607302.36	14343.47	0.00892
$\tilde{\lambda}_3$	3380649.13	3446470.42	3413559.78	32910.64	0.00964
$\tilde{\lambda}_4$	9436746.63	9516020.31	9476383.47	39636.84	0.00418
$\tilde{\lambda}_5$	11957568.67	12067866.95	12012717.81	55149.14	0.00459
$\tilde{\lambda}_6$	17254948.92	17324898.31	17289923.62	34974.69	0.00202
$\tilde{\lambda}_7$	20547852.45	20683224.80	20615538.62	67686.18	0.00328
$\tilde{\lambda}_8$	23940621.60	24062601.45	24001611.53	60989.93	0.00254
$\tilde{\lambda}_9$	27701931.90	27895172.99	27798552.45	96620.55	0.00347
$\tilde{\lambda}_{10}$	33176698.83	33463456.95	33320077.89	143379.06	0.00430
$\tilde{\lambda}_{11}$	34661905.48	34774286.11	34718095.80	56190.31	0.00161
$\tilde{\lambda}_{12}$	40545118.46	41083946.08	40814532.27	269413.81	0.00660
$\tilde{\lambda}_{13}$	51039044.05	51984663.08	51511853.57	472809.52	0.00917

Table (6): Solution of the problem 8.1.3 using the present method

Comparison

The results obtained for problem 8.1.3, using the present method, are compared with the results obtained by Qiu, Chen and Elishakoff (1996); Table (7).

	Lower Bound	Upper Bound	Central Values	Radial Values	Relative Uncertainty
$\tilde{\lambda}_1$	542417.73	795982.85	669200.29	126782.56	0.18945
$\tilde{\lambda}_2$	3203694.23	4208370.82	3706032.52	502338.30	0.13554
$\tilde{\lambda}_3$	8721084.46	8894594.90	8807839.68	86755.22	0.00984
$\tilde{\lambda}_4$	31372412.08	31654701.48	31513556.78	141144.70	0.00447
$\tilde{\lambda}_5$	39003717.83	40388685.94	39696201.89	692484.06	0.01744
$\tilde{\lambda}_6$	66975792.75	68101719.10	67538755.92	562963.18	0.00833
$\tilde{\lambda}_7$	93652364.04	94239659.52	93946011.78	293647.74	0.00312
$\tilde{\lambda}_8$	96645340.33	96958075.71	96801708.02	156367.69	0.00161
$\tilde{\lambda}_9$	115951854.04	116877798.08	116414826.06	462972.02	0.00397
$\tilde{\lambda}_{10}$	260355285.47	260610332.81	260482809.14	127523.67	0.00048
$\tilde{\lambda}_{11}$	480056020.21	480296042.27	480176031.24	120011.03	0.00024
$\tilde{\lambda}_{12}$	689418207.62	689873019.61	689645613.62	227405.99	0.00032
$\tilde{\lambda}_{13}$	818939575.16	819293177.24	819116376.20	176801.04	0.00021

Table (7): Results for problem 8.1.3 by Qiu, Chen and Elishakoff's method

The results for eigenvalues by Qiu, Chen and (1996) for this problem are considerably wider than the exact results. This is most likely because of the existence of interval variation inside the stiffness matrix.

In the eigenvalue step in the IRSA, the computational effort is twice than that required for deterministic analysis. Directional rounding could be used to provide bounds that include the impact of truncation errors.

The additional cost of a true "all interval" method would depend on the computer hardware and the specific method to calculate eigenvalues. In the first step of the IRSA method, only the effects of problem size and initial interval widths determine the behavior of the underlying eigenvalue method. Any interval overestimation will be caused by other steps in the algorithm.

8.2 Examples for Bounds on Dynamics Response

Problem 8.2.1

This example obtains the bounds on dynamic responses for a spring-mass system with fixed supports at both ends with interval uncertainty in the elements' stiffness (Figure (13)).

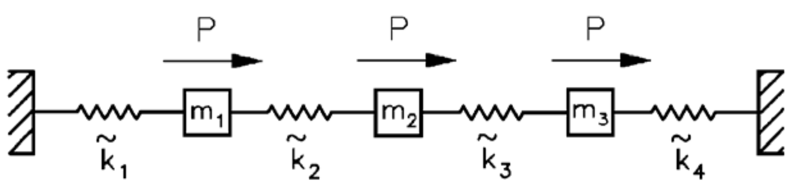

Figure (13): The structure of multi-DOF spring-mass system

The individual element interval stiffness matrices are:

$$\widetilde{K}_1 = \widetilde{K}_2 = \widetilde{K}_3 = \widetilde{K}_4 = ([0.99, 1.01])\begin{bmatrix} +1 & -1 \\ -1 & +1 \end{bmatrix} k$$

The system's stiffness mass matrix is:

$$M = diag(1,1,1)m$$

The excitation is in the form of a suddenly applied proportional constant load as:

$$\{P(t)\} = \begin{Bmatrix} 1 \\ 1 \\ 1 \end{Bmatrix} p$$

The response spectrum for this proportional loading is shown in Figure (14).

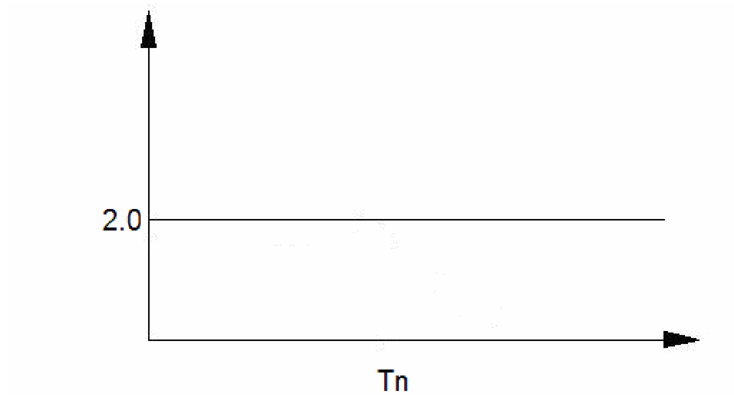

Figure (14): Response spectrum for an external excitation

The problem is solved using the method of interval response spectrum analysis presented in this work and the results are shown in Table (8). For comparison, this problem is solved with two alternate methods:

- Combinatorial analysis: Solution to $2^n = 2^4 = 64$ deterministic problems
- Monte-Carlo simulation: Performing 10^7 simulations using independent uniformly distributed random variables.

Also, the convergence behavior of Monte-Carlo simulation for the displacement of the first node is depicted in Figure(15).

The results for nodal displacements are summarized in Table (8).

	IRSA	Combination	Simulation
$U_{1,\max}$	1.7993	1.7493	1.7491
$U_{2,\max}$	2.4997	2.4577	2.4575
$U_{3,\max}$	1.7993	1.7493	1.7493

Table (8): Solution to the problem 8.2.1

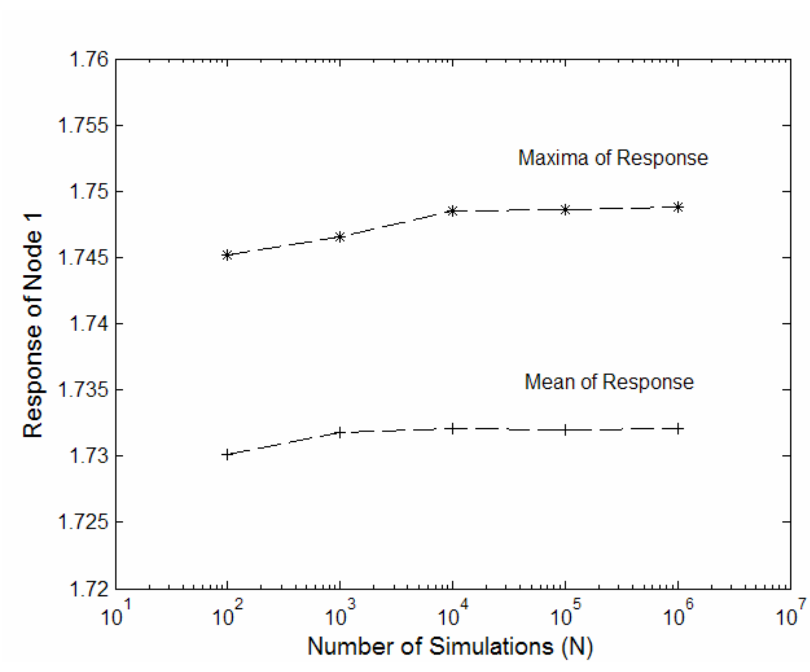

Figure (15): Convergence of Monte-Carlo simulation

Method behavior observations

Problem 8.2.1 is redefined in different ways and solved using IRSA in order to investigate the behavior of the algorithm on following:

Computation time:

Three problems similar to problem 8.2.1 with 3, 4 and 5 DOF using IRSA method and the elapsed time for each problem is recorded and shown in Table (9) and plotted in logarithmic scale in Figure (16).

DOF	Elapsed Time (sec)
3	0.797
5	1.452
6	1.797

Table (9): Computation time of IRSA method for problem 8.2.1

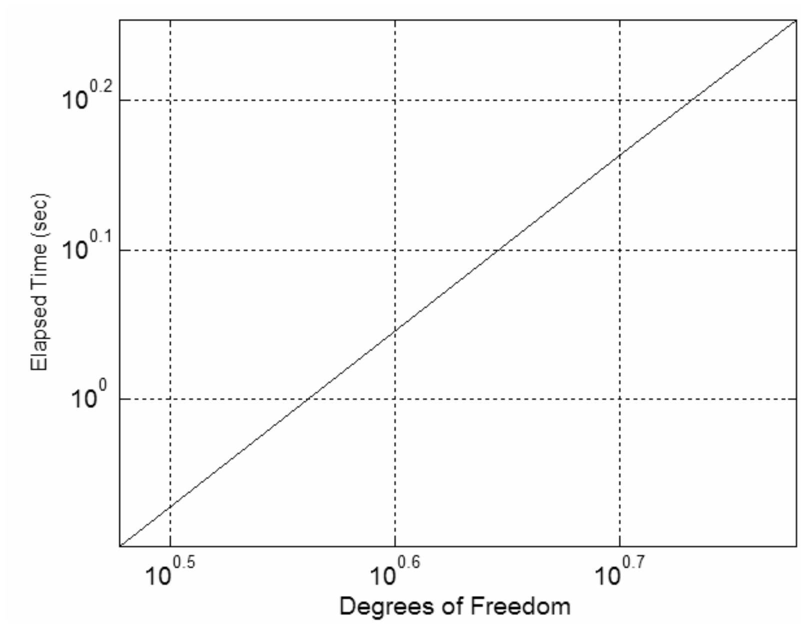

Figure (16): Computation time for IRSA method

The slope of the digram in Figure (15) is about “1.2”. This means that computation time for this problem using IRSA method increases between linear to quadratic with increasing the number of DOF.

Output width as a function of initial width:

Problem 8.2.1 is solved with different input variations in elements’ stiffness and the results are compared with the combinatorial solution. The overestimation in IRSA method is depicted in Figure (17).

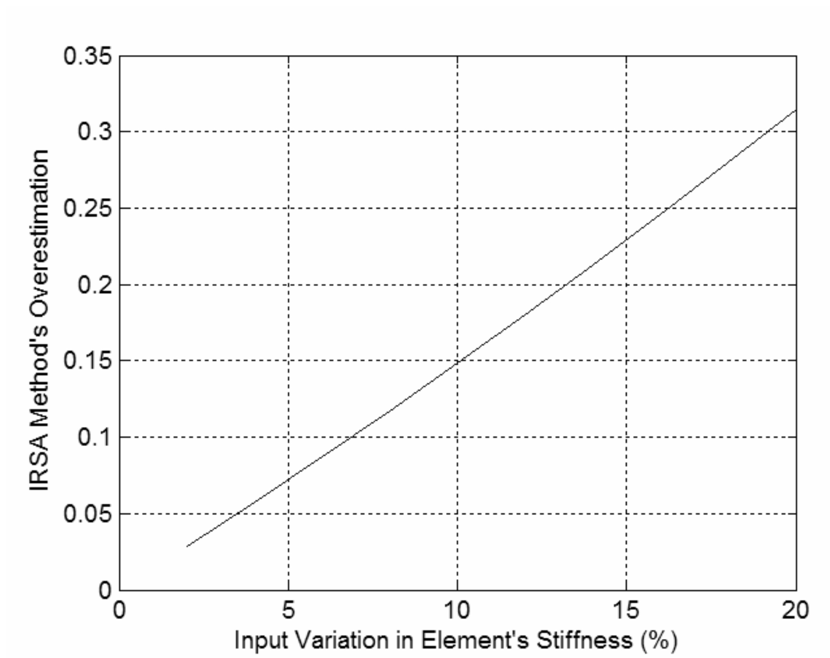

Figure (17): Comparison of output variation for IRSA method with combinatorial solution versus input variation

This shows a linear increase in overestimation of output results for IRSA method compared to the combinatorial solution.

Problem 8.2.2

This example problem solves for the dynamic response a 2-D cross-braced truss system with uncertainty in the modulus of elasticity subjected to an earthquake excitation (Figure (18)).

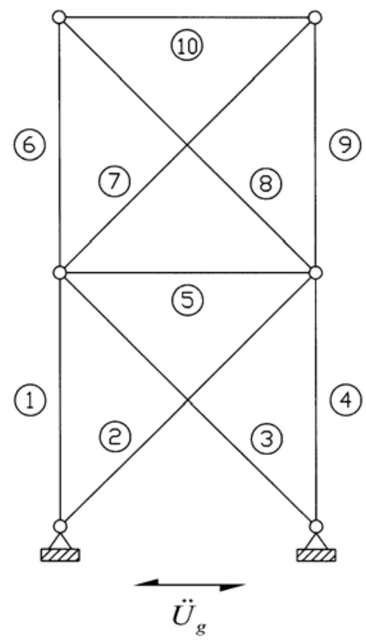

Figure (18): The structure of 2-D cross-braced truss

The cross-sectional area $A = 10 in.^2$, floor load: $0.120 kip / in.^2$, the length for horizontal and vertical members $L = (12) ft$, the Young's moduli E for all elements are $\widetilde{E} = [0.99,1.01]29000 ksi$ and modal damping is $\zeta = 0.02$.

The Newmark Blume Kapur (NBK) design spectra Figure, (2), are used to obtain modal coordinates. The problem is solved using the method of interval response spectrum analysis and the results are shown in Table (10). For comparison, this problem is solved with two alternate methods:

- Combinatorial analysis: Solution to $2^n = 2^{10} = 1024$ deterministic problems
- Monte-Carlo simulation: Performing 10^4 simulations using independent uniformly distributed random variables.

The results for roof lateral displacements ($in.$) are summarized in Table (10).

	IRSA	Combination	Simulation
$U_{\max}$	0.8294	0.8103	0.8103

Table (10): Solution to the problem 8.2.2

Observation

Output width as a function of problem size:

Comparing the results obtained by problems 8.2.1 and 8.2.2 shows that the overestimation of IRSA method in output results does not increase with increasing the number of elements and DOF.

CHAPTER IX

CONCLUSIONS

- A finite-element based method for dynamic analysis of structures with interval uncertainty in structure's stiffness or mass properties is presented.
- In the presence of any interval uncertainty in the characteristics of structural elements, the proposed method of interval response spectrum analysis (IRSA) is capable to obtain the nearly sharp bounds on the structure's dynamic response.
- IRSA is computationally feasible and it shows that the bounds on the dynamic response can be obtained without combinatorial or Monte-Carlo simulation procedures.
- The solutions to only two non-interval eigenvalue problems are sufficient to bound the natural frequencies of the structure. Based on the given mathematical proof, the obtained bounds on natural frequencies are exact and sharp.
- Computation time for the algorithm increases between linear to quadratic with increasing the number of degrees of freedom.
- Some conservative overestimation in dynamic response occurs because of linearization in formation of bounds of mode shapes and also, the dependency of intervals in the dynamic response formulation. These are the expected cause of loss of sharpness in the interval results.

- The overestimation of output results for IRSA method linearly increases with increasing the number of degrees of freedom in comparison with the combinatorial solution.
- The solution of the solved problems for dynamic response indicates that the output overestimation does not increase as the problem size increases.
- The computational efficiency of the proposed method makes IRSA an attractive method to introduce uncertainty into dynamic analysis.

REFERENCE

Alefeld, G. & Herzberger, J., 1983 "*Introduction to Linear Computation* " , NewYork: Academic Press.

Anderson, A.W., et al 1952 "*Lateral Forces on Earthquake and Wind*", Trans. ASCE, Vol. 117, p. 716.

Archimedes (287-212 B.C.); by Heath, T.L., 1897 "*The Works of Archimedes*", Cambridge, Cambridge University Press.

Bellman, Richard, 1960 "*Introduction to Matrix Analysis* " , McGrawHill, New York.

Biggs, J. M.,1964 "I*ntroduction to Structural Dynamics*" McGraw-Hill, Inc.

Biot, M. A., 1932 "*Vibrations of Buildings during Earthquake*", Chapter II in Ph.D. Thesis No. 259 entitled "*Transient Oscillations in Elastic System*", Aeronautics Department, Calif. Inst. of Tech., Pasadena, California, U.S.A.

Clough, R.W., & Penzien, J. 1993 "*Dynamics of Structures*", McGraw-Hill, New York.

Dennis Jr. , D.E. Jr. & Schnabel, R.B. 1983 "*Numerical Methods for Unconstrained Optimization and Nonlinear Equations*" Prentice-Hall, Englewood Cliffs.

Dief, A., 1991 "*Advanced Matrix theory for Scientists and Engineers*",pp.262-281. Abacus Press (1991)

Dwyer, P. S., 1951 "*Linear Computations* " , New York: John Wiley.

Housner, G. W., 1959 "*Behavior of Structures During Earthquake*" Proc. ASCE Vol. 85, No. EM 4 p. 109.

Hudson, D. E., 1956 "*Response Spectrum Techniques in Engineering Seismology*" Proc. World Conf. on Earthquake Eng. Earthquake Engineering Research Institute, Berkeley, California.

Gasparini, Dario A., 2003, Class-notes for ECIV-424 "*Structural Dynamics*". Department of Civil Engineering, Case Western Reserve University, Cleveland, Ohio.

Qiu, Z. P., Chen, S. H., and Elishakoff, I. 1995, "*Natural frequencies of structures with uncertain but non-random parameters*", J. Optimization Theor. Appl. 86, 669-683 (1995).

Qiu, Z. P., Chen, S. H., and Elishakoff, I. 1996, "*Non-probabilistic Eigenvalue Problem for Structures with Uncertain Parameters via Interval Analysis*",Chaos, soliton and fractals,7, 303-308 (1996).

Moore, Ramon E., 1966 "*Interval Analysis*", Prentice Hall, Englewood, NJ.
Newmark, N. M., 1962 "*A Method of Computation for Structural Dynamics*", Trans. ASCE, Vol. 127, pt. 1, pp. 1406-1435.

Muhanna, Rafi L. & Mullen, Robert L., 2001. "*Uncertainty in Mechanics Problems-Interval-Based Approach*". Journal of Engineering Mechanics June-2001, pp.557-566.

Muhanna, R. L. and Mullen, R. L., "*Formulation of Fuzzy Finite Element Methods for Mechanics Problems*", Computer-Aided Civil and Infrastructure Engineering, 14, pp. 107-117, 1999.

Mullen, Robert L., 2003, Class-notes for ECIV-420 "*Finite Element Analysis I*". Department of Civil Engineering, Case Western Reserve University, Cleveland, Ohio.

Newmark, N. M., Blume, J. A. and Kapur, K. K. 1973 "*Seismic Design Spectra for Nuclear Power Plants*". J. Power Division, Proc ASCE, Vol. 99, No. P02, 287-303.

Neumaier, Arnold, 1990 "*Interval Methods for Systems of Equations*", Cambridge University Press, Cambridge.

Looney, C. T. G., 1954 "*Behavior of Structures Subjected to a Forced Vibration*", Proc. ASCE, Vol. 80, Separate No. 451.

Rosenblueth, E. & Bustamente, J. I., 1962 "*Distribution of Structural Response to Earthquakes*", Proc. ASCE, Vol. 88, No. EM 3 p. 75.

Sunaga, T., 1958 "*Theory of an Interval Algebra and its Application to Numerical Analysis*" RAAG Memoirs II 2, 547-565. Tokyo, Japan.

Stewart, G.W. & Sun, Ji-Guang, 1990 "*Matrix perturbation theory*" Academic Press, Boston, MA.

Strang, Gilbert, 1976 "*Linear Algebra and its Applications*", Massachusetts Institute of Technology.

Trefethen, L. N. & Bau III, D., 1997 "*Numerical Linear Algebra*", SIAM.

Veletsos, A. S. & Newmark, N. M., 1957 "*Natural Frequencies of Continuous Flexural Members*", Trans. ASCE, Vol. 122, p. 249.

Young, R. C., 1931 "*The Algebra of Many-Valued Quantities*" Mathematics Annalen 104, 260-290.